Spring 5-2008

Reverse Recruitment: Activation of Yeast Genes at the Nuclear Periphery

Terry Marvin Haley
University of Southern Mississippi

The University of Southern Mississippi

REVERSE RECRUITMENT: ACTIVATION OF YEAST GENES AT THE NUCLEAR PERIPHERY

by

Terry Marvin Haley

A Dissertation
Submitted to the Graduate Studies Office
of The University of Southern Mississippi
in Partial Fulfillment of the Requirements
for the Degree of Doctor of Philosophy

Approved:

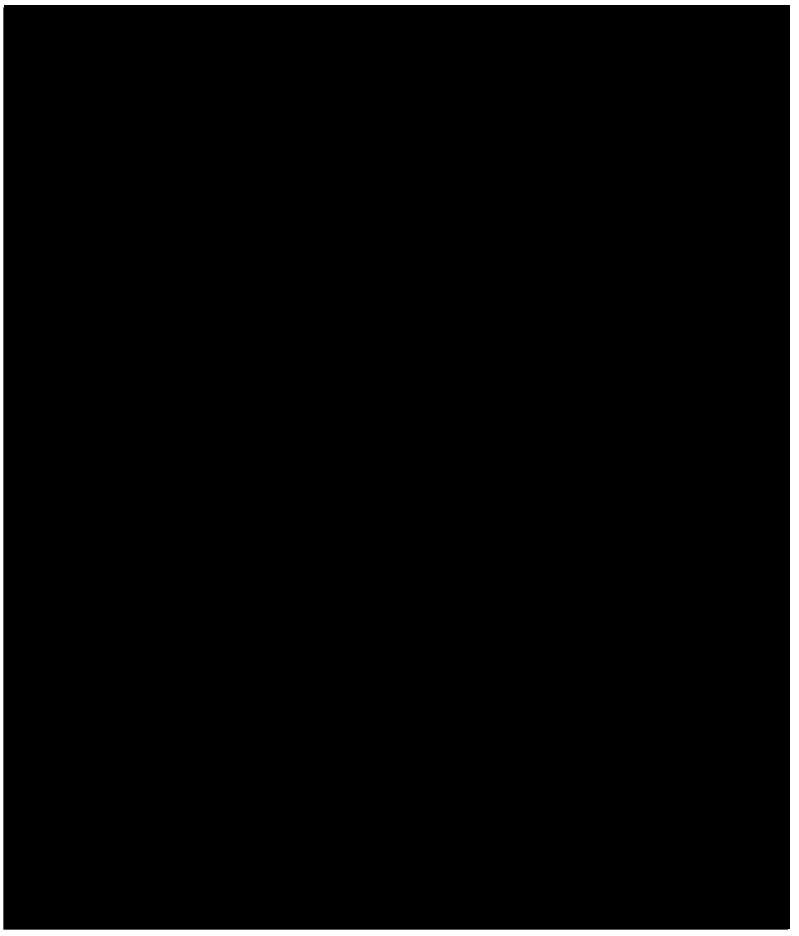

May 2008

The University of Southern Mississippi

REVERSE RECRUITMENT: ACTIVATION OF YEAST GENES AT THE NUCLEAR PERIPHERY

by

Terry Marvin Haley

Abstract of a Dissertation
Submitted to the Graduate Studies Office
of The University of Southern Mississippi
in Partial Fulfillment of the Requirements
for the Degree of Doctor of Philosophy

May 2008

ABSTRACT

REVERSE RECRUITMENT: ACTIVATION OF YEAST GENES

AT THE NUCLEAR PERIPHERY

by Terry Marvin Haley

May 2008

The regulation of genes at the nuclear periphery is an evolutionarily conserved phenomenon in eukaryotes. The reverse recruitment model of transcriptional activation postulates that genes are activated by moving to and contacting transcription machinery located at subnuclear structures. In *Saccharomyces cerevisiae* it has been reported that this platform for gene regulation may reside at the nuclear periphery. To test this hypothesis, I utilized a GFP-gene tagging technique, which uses LacI-GFP to visualize a tandem array of its DNA-binding sequence, to monitor localization of *SUC2* and *GAL1*. I found that both genes preferentially localized to the nuclear periphery when transcriptionally active. By developing an *in vivo* single cell reporter assay, I simultaneously monitored gene location and expression of a GFP-Ras2 reporter and found that, when induced, cells with perinuclear *GAL* genes activated transcription 10 minutes before cells with genes localized to the nucleoplasm. Thus, interaction with the nuclear periphery correlates with more rapid initiation. Further, the *GAL1* gene can anchor in response to galactose, even when transcription is blocked, suggesting that genes move to the nuclear periphery prior to transcriptional initiation. I also show that gene localization to the nuclear periphery correlates with defects in regulation caused by the removal of *SUC2* and *GAL1* regulatory factors. Strikingly, these factors can be

biochemically purified with the perinuclear compartment. Further, I report here that components of the transcriptional pre-initiation complex are localized to the nuclear periphery in the presence or absence of transcription. This suggests that there is a highly organized subnuclear architecture that facilitates gene regulation at the nuclear periphery.

Interestingly, I saw that the archetypal transcriptional activator Gal4 exhibits a quantifiable difference in its subnuclear mobility that correlates with its function. For example, induced Gal4 shifts to a more slowly mobile form. I hypothesize that this shift may be the result of interaction with perinuclear transcription factories and that the well characterized dimerization and activation domains of Gal4 play a role in this tethering. Finally, I propose a model by which chromatin structure can influence gene movement to the nuclear periphery through the dynamic conversion between heterochromatin and euchromatin.

ACKNOWLEDGEMENTS

I would like to acknowledge several exceptional individuals that have helped me throughout my doctoral work. First and foremost, I'd like to thank my advisor, Dr. George Santangelo for his commitment of time and patience in teaching a former computer scientist the intricacies, and challenges, of biomedical research. I would like to also thank the members of my dissertation committee, Dr. Kelly Tatchell, Dr. Robert Bateman, Dr. Mohamed Elasri and Dr. Youping Deng, for their excellent guidance and suggestions regarding my research. I'm especially grateful to Dr. Kristine Willis who has graciously donated her time and effort in assisting in manuscript preparations and experimental suggestions. I'd like to also thank the current and past members of the Santangelo lab, in particular Dr. David Buford for his biochemical expertise shown here in Figures 6B, 11, 12, 13 and 16C, Dr. Nayan Sarma for his expertise in ChIP and invertase assays shown here in Figure 5C and Table 3. Again, I'd like to thank Dr. George Santangelo specifically for helping to quantitate the data shown in Figures 10 & 16B, which was done while I was in the Caribbean on my honeymoon. For their support and unending encouragement, I'd like to thank my friends and family. Lastly, I owe a great deal of thanks to my love and companion, Kellie Barbara Haley.

TABLE OF CONTENTS

LIST OF ILLUSTRATIONS

Figure

LIST OF TABLES

Table

CHAPTER I

BACKGROUND AND SIGNIFICANCE

Regulation of gene transcription is a key feature of developmental, homeostatic and oncogenic processes; misregulated genes are often responsible for developmental diseases and cancer. The unicellular yeast *Saccharomyces cerevisiae* continues to be a valuable model organism with which to study eukaryotic gene regulation, in particular because it allows integration of a variety of independent approaches (e.g. biochemistry, cell biology and genetics). Numerous features of transcriptional regulation are strongly conserved in yeast and human cells. For example, human TFTC (TBP-free TAF-containing histone acetyltransferase) and yeast SAGA (Spt-Ada-Gcn5 histone acetyltransferase) are conserved with respect to function, overall structure and subunit composition. This is particularly striking because each of these complexes contains twenty or more different polypeptides. These human and yeast co-activators are therefore likely to regulate transcription via a common mechanism (Brand *et al.* 1999). Thus, the easily manipulated yeast model system has great relevance to understanding homologous systems in higher eukaryotes.

The eukaryotic nucleus is highly organized with respect to gene regulation and RNA processing. Nuclear substructures seem to be particularly important in facilitating or regulating gene expression. In mammalian cells, RNA polymerase II assembles and localizes to lumenal Cajal bodies as active sites of transcription (Platani *et al.* 2002). Additionally, promyelocytic leukemia (PML) bodies regulate apoptosis in response to DNA damage (Boe *et al.* 2006). Lacking these lumenal structures, yeast gene expression appears to occur via movement of active genes to the nuclear periphery soon after

induction (Brown and Silver 2007). While a functional role for nuclear organization is changing the way in which we view the regulation of gene expression, much remains to be eludicated for the development of a clear and accurate model of transcription in three-dimensional space.

It is becoming clear, with the growing body of evidence correlating gene localization with transcription state, that the nuclear lumen is comprised of an ordered collection of spatial relationships. A model to describe gene regulation by relocation to a specific subnuclear compartment for activation was reported as early as 1985 with the concept of gene gating (Blobel 1985). This model postulated that remodeled genes targeted for activation localized to the nuclear pore complexes. Interestingly, the first report linking transcriptional activation with the nuclear periphery was published that same year (Hutchison and Weintraub 1985). However, because of limitations in technology, at the time it was difficult to rationalize this proposed hypothesis. Conversely, three years later, the recruitment model of transcription was published, which postulates that Brownian motion acts upon regulatory elements that then come into contact with their target genes for activation. Since this model complimented what was currently being elucidated of gene regulation using the then modern techniques, recruitment became the accepted paradigm for gene activation (Ptashne 1988). However, work by several eukaryotic labs has recently called the recruitment model of gene activation into question.

Only recently gene localization to the periphery in the context of activation has become center stage as a rapidly growing list of yeast genes has been shown to exhibit this behavior: these include *INO1* (Brickner and Walter 2004), *GAL1-10* (this work;

Casolari et al. 2004), *GAL2* (Dieppois *et al.* 2006), *HSP104* (Dieppois *et al.* 2006), *HXK1* (Taddei *et al.* 2006) and *SUC2* (this work; Sarma *et al.* 2007) to name a few. The information provided by these recent observations was made possible with the modern advances in cell biology techniques (see below). These findings have provided significant new insights into gene regulation in the context of a three dimensional, organized nucleus vs. a mixed 'soup' of complexes and chromatin.

A number of models have been developed in an attempt to explain this aspect to gene activation in yeast. Mentioned above, the gene gating model postulates that the nuclear pore complexes are a likely site of gene regulation based on the relationship between NPC distribution within the nuclear membrane and chromatin organization (Blobel 1985). More recently, models such as nucleoporin promoter interation (Nup-PI; Schmid *et al.* 2006)), gene recruitment (Brickner and Walter 2004) and reverse recruitment (Menon *et al.* 2005) have placed the key component of gene localization to the periphery with the NPC as well. However, they differ in the mechanistic details of How, Why and When gene relocalization occurs. The Gasser and Silver labs have reported that gene movement to the periphery follows the initial round of transcription of a target gene and that the first mRNA product facilitates this motion (reviewed in (Akhtar and Gasser 2007; Drubin *et al.* 2006; Taddei *et al.* 2006), though they test this indirectly. Conversely, our lab and the Brickner lab report that gene movement to the periphery occurs in the absence of transcription for *GAL1* and *INO1*, postulating that initiation occurs at the nuclear periphery (this work; Brickner *et al.* 2007). These distinct hypotheses describing gene localization in the context of regulation will need to be

answered through more direct observations. Specifically, the field needs to address the initial round of transcription and the mechanism of gene movement.

To better understand the relationship between transcriptional activation and the subnuclear localization of genes and their regulators, I have undertaken a largely cell biological approach to address several questions of interest: A) Do yeast nucleoporins associate tightly within the NPC and how does that relate to other nuclear factors? B) How do environmental signals (i.e. for repression or activation) affect subnuclear localization of regulators and their target genes? To address this, I have utilized the well characterized glucose-repressed gene *SUC2* and the galactose-induced gene *GAL1*. C) How do mutations in the well-characterized modular domains of a transcriptional activator (i.e. the activation domain or DNA-binding domain) affect its localization, mobility and ability to function? For this analysis I examine targeted deletions in the prototypical Gal4 activator.

In the remainder of this chapter I will review the current literature for topics pertinent to the understanding of this work.

Nuclear Substructure and Chromatin Dynamics

It is well established that the eukaryotic nucleus has an ordered substructure that facilitates gene regulation (see above; reviewed in O'Brien *et al.* 2003)). For example, in mammalian cells, it has been known a long time that chromosomes reside within distinct regions of the nucleus called territories (Lichter *et al.* 1988; Pinkel *et al.* 1988). These territories contain highly condensed regions of inactive chromatin. Active genes translocate to less dense interchromatin spaces to interact with PML or Cajal bodies for transcription. The resulting RNA is then modified in these regions prior to export or

further processing at the nucleolus (Verschure *et al.* 1999). Present research in yeast has yet to identify corresponding structures analogous to PML and Cajal bodies or structures resembling chromosomal territories. However, it is becoming clear that subnuclear organization exists and correlates with gene expression (see below).

In yeast, silent chromatin resides at the nuclear periphery (Gotta and Gasser 1996). Though the mechanism of peripheral anchoring remains unknown, yKu80, Esc1 and Sir4 have all been implicated to contribute to this process (Taddei *et al.* 2004). This example of subnuclear organization led researchers to adopt the reasonable but naïve assumption that the yeast nuclear periphery is a "silenced" compartment. However, as mentioned above, the nuclear pore complex (NPC) has been an intense focus of research in gene activation.

Gene Regulation in Saccharomyces cerevisiae

Transcription of the yeast protein-encoding genes is accomplished by RNA polymerase II (Pol II). The Pol II complex is composed of twelve subunits encoded by the RNA polymerase (*RPO*) genes. Many of these subunits have homologous counterparts in RNA polymerase I and III; others are common subunits shared between all three polymerases. Additional factors are needed for accurate gene transcription by Pol II: TBP (TATA-binding protein), TFIIB, TFIID, TFIIE, TFIIF and TFIIH. These factors have been reviewed extensively (Hampsey 1998) and will be considered here as part of the general transcriptional machinery referred to as Pol II.

In eukaryotic cells, gene expression has been described as a stepwise process beginning with an activator and culminating in the engagement of the Pol II complex (Figure 1A); however this model has been difficult to verify and is no longer universally

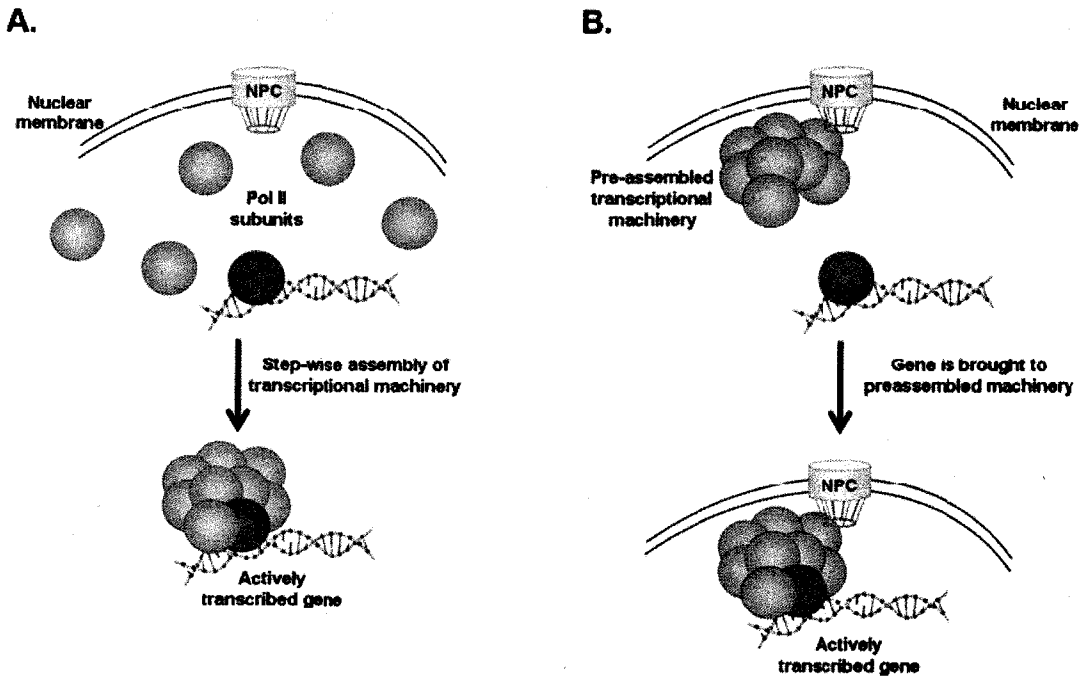

Figure 1. Two models for transcriptional activation. (**A**) The diffusion-based recruitment model emphasizes stepwise assembly of the transcriptional machinery on the DNA, without accounting for nuclear substructures. (**B**) The reverse recruitment model is based on organization of the transcriptional machinery via nuclear substructures, such as the nuclear pore complex (NPC). In this model, DNA is the mobile element and is recruited to the nuclear periphery to be activated.

accepted. Additionally other complexes have been identified as global regulators that enhance transcription via chromatin remodeling; these include the Mediator, Swi/Snf and SAGA complexes. The inclusion of these intermediary complexes unique to eukaryotes is thought to enable more complex gene attenuation for processes such as differentiation and development (Kornberg 2005).

Mediator Complex

The Mediator complex was discovered due to its ability to relieve transcriptional squelching, or the interference of an activator caused by overexpression of an unrelated activator (Gill and Ptashne 1988). The interference was originally attributed to the sequestration of a required factor or Pol II itself by the overexpressed activator. However,

this interference could not be overcome in *in vitro* experiments by an excess of those purified factors, but instead could be overcome by a particular fraction from yeast extracts (Kelleher *et al.* 1990). This activity was deemed Mediator and the corresponding complex was isolated four years later (Kim *et al.* 1994). Comprised of twenty-one subunits, Mediator interacts with the C-terminal domain of Pol II's largest subunit, Rpb1 (Myers *et al.* 1998). Current models put Mediator as the bridge between the Pol II complex and DNA-bound transcriptional activators, since its effect on transcription was isolated to the upstream activating sequences (UAS) that are known to be activator-bound under induced conditions (Park *et al.* 2000). Together, the Mediator and Pol II complexes are often collectively referred to as the Pol II holoenzyme (Myers *et al.* 1998).

SAGA complex

In yeast, Gcn5 along with several Spt and Ada proteins constitute the Spt-Ada-Gcn5 acetyltransferase (SAGA) complex. Sgf73 was recently identified as a new component of SAGA that is required for association with the UAS of target genes in an activator-dependent manner. The SAGA complex utilizes acetyl-CoA for histone acetylation and is required for the proper expression of 10% or more of the yeast genome (Lee *et al.* 2000). Gcn5 histone acetyltransferase (HAT) performs its enzymatic function by transferring the acetyl group from acetyl-CoA to lysine sidechains of the histone core proteins. This enzymatic activity hyperacetylates the target histones and is often correlated with actively transcribed genes (Sterner and Berger 2000).

Swi/Snf chromatin remodeling complex

The Swi/Snf remodeling complex contains eleven subunits (Sudarsanam and Winston 2000). DNA-bound transcriptional activators (Schwabish and Struhl 2007), as

well as histone acetylation by the SAGA complex, facilitates the interaction of the Swi/Snf complex with nucleosomes at gene promoters (Chandy *et al.* 2006). The Swi/Snf complex is then capable of shifting or evicting local nucleosomes to promote transcription initiation and elongation (Schwabish and Struhl 2007). A defect in Swi/Snf function causes a drop in activator-dependent gene expression (Qiu *et al.* 2004).

Activation by Recruitment

Recruitment has been the generally accepted model to explain how eukaryotic gene activation occurs. The recruitment model (summarized in Figure 1A) theorizes that gene activation occurs when a DNA-bound activator attracts components of the general transcription machinery to the UAS of a target gene in a step-wise fashion (Ptashne and Gann 1997). Recruitment is based largely upon an experiment that fused the DNA-binding domain (DBD) of the strong activator Gal4 directly to a component of the Pol II holoenzyme (Barberis *et al.* 1995); this fusion could activate high levels of transcription of the Gal4 target genes. This phenomenon, called activator bypass, supported the idea of the machinery being recruited to target genes for expression in a DNA-bound activator dependent fashion. Corresponding fusions of the activation domain (AD) of Gal4 failed to activate transcription. These results led to the idea that the AD functions as the recruitment surface for the Pol II holoenzyme, while the DBD provides a specific contact surface with the DNA (Keaveney and Struhl 1998).

Since the development of the recruitment model in the late 1980's, discrepancies have been identified. For one, the bypass experiment described above, where it was presumed that the DNA binding domain was fused to a single holoenzyme subunit was in fact fused to a Mediator component (Kornberg 2005). However, subsequent experiments

have suggested that Mediator precedes the Pol II complex in associating with the UAS of target genes (Cosma *et al.* 1999). Another discrepancy with the recruitment model is the Rap1 transcriptional regulator. When the activity of Rap1-Gal4DBD or Rap1-LexA fusion proteins are measured, Rap1 activation appears surprisingly weak (Santangelo 2006). However, this is not representative of Rap1 being a weak activator since mutation of its canonical binding sequence causes a 10 to 20 fold decrease in activation of its native target genes (Tornow *et al.* 1993). The recruitment model can not easily account for the observations.

Activation by Reverse Recruitment

A growing body of evidence is emerging that supports an alternative to the traditional paradigm of recruitment; this alternative is termed 'reverse recruitment' (Brown and Silver 2007; Menon *et al.* 2005; Santangelo 2006; Sarma *et al.* 2007). The inspiration of reverse recruitment began with an SGA analysis that showed a genetic link between the glycolytic activator Gcr1 and a dozen nucleoporins (Menon *et al.* 2005). This result begged the question of how the NPCs might play a role in regulation. Subsequent experiments showed that nucleoporins themselves can activate transcription of a reporter when fused with a LexA DNA-binding domain (Menon *et al.* 2005). These results allowed us to then develop a new model for gene regulation.

The reverse recruitment model stipulates that to be transcribed DNA is brought to an active region, such as the nuclear periphery, rich in pre-assembled transcriptional machinery (Figure 1B), rather than the machinery components diffusing randomly throughout the nucleoplasm and assembling *de novo* on each active promoter. Thus, unlike the recruitment model, this model takes into account the relationship between

nuclear substructure and gene regulation. A culmination of work from many labs has shown reverse recruitment to be a viable model of expression for Rap1/Gcr1 (Menon *et al.* 2005), glucose repressed genes (Sarma *et al.* 2007), galactose inducible genes (this work; Cabal *et al.* 2006; Drubin *et al.* 2006; Taddei *et al.* 2006) and the unfolded protein response genes (Brickner and Walter 2004).

Glucose repression of SUC2

Glucose repression is a robust and well studied pathway in yeast by which signal transduction blocks the expression of ~1000 genes. As in higher eukaryotes, the Ras/cAMP-dependent protein kinase A (PKA) initiates a transcriptome-wide glucose response (Santangelo 2006). In response to this signal, Hxk2, Ssn6 and DNA-binding Mig1 participate in the transduction pathway that blocks transcription of glucose repressed genes (Carlson 1999). Transcriptional inhibition is relieved in the absence of the glucose signal when Mig1 is evicted from the nucleus as a consequence of phosphorylation by the Snf1 kinase complex (Sarma *et al.* 2007). *SUC2*, the gene encoding the invertase enzyme, has been a model for the study of repression. Interestingly, despite the wealth of details known about its transcriptional repression in response to glucose, a DNA-bound activator for *SUC2* has yet to be identified.

Inducible expression of GAL1

Although it is unclear whether or not *SUC2* has an exclusive activator, *GAL* gene expression requires the well studied transcriptional activator Gal4. Induction by galactose requires a three component switch mechanism, Gal3, Gal80 and Gal4 (see below). In the absence of galactose this switch works to inhibit activation of the *GAL* genes.

Conversely, in the presence of galactose, this switch allows for the productive interaction of Gal4 with its canonical target genes (Lohr *et al.* 1995).

Gal80 repressor has been reported to bind directly to a short sequence within the Gal4 activation domain spanning residues 850 to 874 (Ma and Ptashne 1987). This inhibitory complex does not prevent Gal4 from binding its target sequences, but inhibits Gal4 activation of target genes. The addition of galactose to cells is sufficient to overcome Gal80's sequestration of Gal4. Though the specific mechanism has yet to be elucidated, it has been shown that Gal3 or the homologous Gal1 (Sil *et al.* 1999), competitively binds Gal80 in the presence of galactose, releasing Gal4 for gene activation (Pilauri *et al.* 2005).

Galactose Activator Gal4

General activator components

Transcriptional activators are thought to minimally require the DNA-binding domains (DBD) and activation domain (AD) modules (Ding and Johnston 1997; Ptashne and Gann 1997; Triezenberg 1995). Since the DBD structure in each activator defines the specific sequences it targets in genomic DNA, the initial expectation was that a determination of AD structure would rapidly uncover the mechanism of AD function (Mitchell and Tjian 1989; Ptashne 1988). Unfortunately this has not been straightforward. Although ADs have been shown to adopt secondary structure upon interaction with binding partners (usually an amphipathic α–helix; Ferreira *et al.* 2005; Sugase *et al.* 2007), under physiological conditions ADs are intrinsically unstructured, highly flexible random-coil domains (Triezenberg 1995; Wright and Dyson 1999). Thus, though the primary AD of Gal4 (Gal4AD1; Figure 2) functions in all eukaryotes tested (Ptashne and Gann 1990), it

shows no apparent sequence conservation with respect to ADs in other activators, even within the *S. cerevisiae* Gal4 superfamily (MacPherson *et al.* 2006; Schjerling and Holmberg 1996).

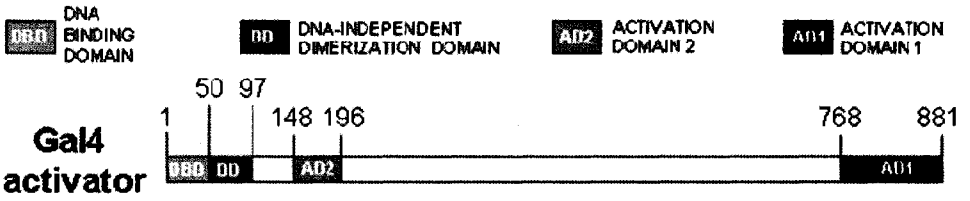

Figure 2. The modular structure of Gal4. Separable functions are encoded by the DNA binding domain (DBD), the DNA-independent dimerization domain (DD) and the C-terminal activation domain (AD1). Removal of AD1 revealed the existence of a second, less powerful activation domain (AD2). The region between residues 196 and 768 plays at most a minor role in Gal4 function (Ding and Johnston 1997; Ma and Ptashne 1987).

Gal4 structural anatomy

Analysis of the transcriptional regulator Gal4 in *S. cerevisiae*, which stimulates expression of genes required for galactose metabolism, was important in establishing both the function of DNA-bound activators and the prevalent paradigm of eukaryotic gene induction (Johnston 1987; Johnston *et al.* 1986; Zaman *et al.* 1998). All 50+ members of the Gal4 superfamily in *S. cerevisiae* are thought to share the modular structure of Gal4 (Figure 2). These proteins typically bind a pair of CGG nucleotide triplets as a homodimer and have separable DNA binding, dimerization (DD), and activation domains. Gal4 actually contains two ADs. The primary AD (AD1 in Figure 2) accounts for the majority of its activation, while the secondary AD (AD2 in Figure 2) has weaker activity. Crystal structures have been determined for the Zn-Cys binuclear cluster-type DBD in Gal4 (Marmorstein *et al.* 1992) and the other best-characterized members of the Gal4 superfamily, including Put3, Hap1, Ppr1 and Leu3 (MacPherson *et al.* 2006). Swapping the zinc cluster motif (residues 8-40 in Gal4) of one activator for

another does not affect DNA targeting; binding specificity is thought to be derived from the adjacent linker region (residues 41-49 in Gal4; MacPherson *et al.* 2006; Marmorstein *et al.* 1992). The dimerization domain in Gal4 (Gal4DD; residues 50-97) augments, but is not required for, specific binding of Gal4 dimers to the 17mer target in DNA, UAS_G (Carey *et al.* 1989; Keegan *et al.* 1986).

Fluorescent Proteins in Cell Biology

The Green Fluorescent Protein (GFP) was isolated from the jellyfish *Aequoria victoria* and has become one of the most widely utilized proteins in cell biology (Tsien 1998). Its discovery revolutionized the field as the fundamental cornerstone of *in vivo* fluorescent techniques. The ability of GFP to form a highly visible and stable chromophore is an exceptionally useful tool. Further, since GFP has no special environmental folding requirements, it is amenable to expression in various systems and can be fused to other proteins with minimal effect on a host organism. As a result, GFP has been used for a plethora of cell biology experiments from protein localization (Huh 2003) to the study of chromosome dynamics (Drubin *et al.* 2006).

Solving the crystal structure of GFP allowed for a closer analysis of the chromophore (Perozzo *et al.* 1988). In order to absorb energy and subsequently emit light, the chromophore must undergo fluor maturation. Maturation describes the process that begins with the translation of the mRNA message to its final folded and fluorescing state. Cyclization of the amino acid backbone to form the chromophore is the rate limiting step of this process (Sniegowski *et al.* 2005). This internal component is encapsulated within an eleven stranded beta barrel. Fully folded, the GFP protein absorbs light at 488nm and emits light at 505nm (Heim *et al.* 1994).

With the crystal structure of GFP solved, a targeted mutational analysis was begun to identify the components necessary for fluorescence (Li *et al.* 1997). Through these experiments, many mutant variants were developed with a range of properties: enhanced chromophore brightness, stability and cyclization to name a few (Verkhusha *et al.* 2001). For example, the original isolates of GFP have a maturation rate of four hours (Kolb *et al.* 1996), a potential limiting factor for expression reporting (Yeh *et al.* 1995). The optimization imposed on GFP provided alternatives whose maturation rates were greatly reduced (Verkhusha *et al.* 2001). These improvements in maturation rate have enabled protocols to be performed that were otherwise impossible. Another development resulting from mutational analysis was variants that emitted at different wavelengths. Today, the fluorescent color palette is rich with over 20 individual fluorescent proteins available, each with their own photo-properties (Stewart 2006).

Photobleaching

Building further upon the growing number of cell biological tools, it was contrived to use bleaching techniques to explore a protein's Brownian mobility within its cellular compartment (Lippincott-Schwartz *et al.* 2003). The technique uses excessive excitation to extinguish chromophores within a selected region of a fluorescent population. After bleaching, the rate at which fluorescence is recovered or lost can be measured as the variants equilibrate within their subcellular compartment. The rate and extent to which this occurs can be quantified to elucidate the kinetic properties of a protein (Rabut *et al.* 2004).

Fluorescence Recovery After Photobleaching (FRAP)

The FRAP technique measures the recovery of fluorescence within a small region of interest (Figures 3A & B). This region is then photo-bleached with a high intensity light source and subsequently observed over time with a corresponding light source of low intensity (Figures 3C & D). The resulting fluorescence recovery curve can be used to quantitate protein properties of diffusion and immobility (Figure 3E). Factors that can affect this recovery include size of the tagged protein, density of organic material and structural interactions. Hence, the FRAP technique is suited to analyze proteins that loosely associate with structures or are constituents of mobile complexes (reviewed in (Lippincott-Schwartz *et al.* 2003).

inverse Fluorescence Recovery After Photobleaching (iFRAP)

iFRAP represents the converse of FRAP as implied by the name. With iFRAP, the fluorescent population is separated into two regions: the area to be bleached and the area to be observed (Figures 4A & B). The region to be bleached will encompass the majority of the fluorescing population, while the smaller unbleached region will be observed for fluorescence loss over time (Figures 4C & D). Quantitation of the loss of fluorescence yields the rate of structural dissociation (Figure 4E). This resulting curve can be used to determine a protein's 'residence time' within a structure, which is designated as the time it takes for 50% of fluorescence loss to occur. Proteins that are tight constituents of an immobile structure will exhibit a higher residence time as opposed to a loosely bound or freely diffusing protein whose fluorescence diminishes rapidly. Whereas FRAP measures a protein's freedom of mobility, iFRAP quatitates a protein's structural retention (describe in (Dundr and Misteli 2003).

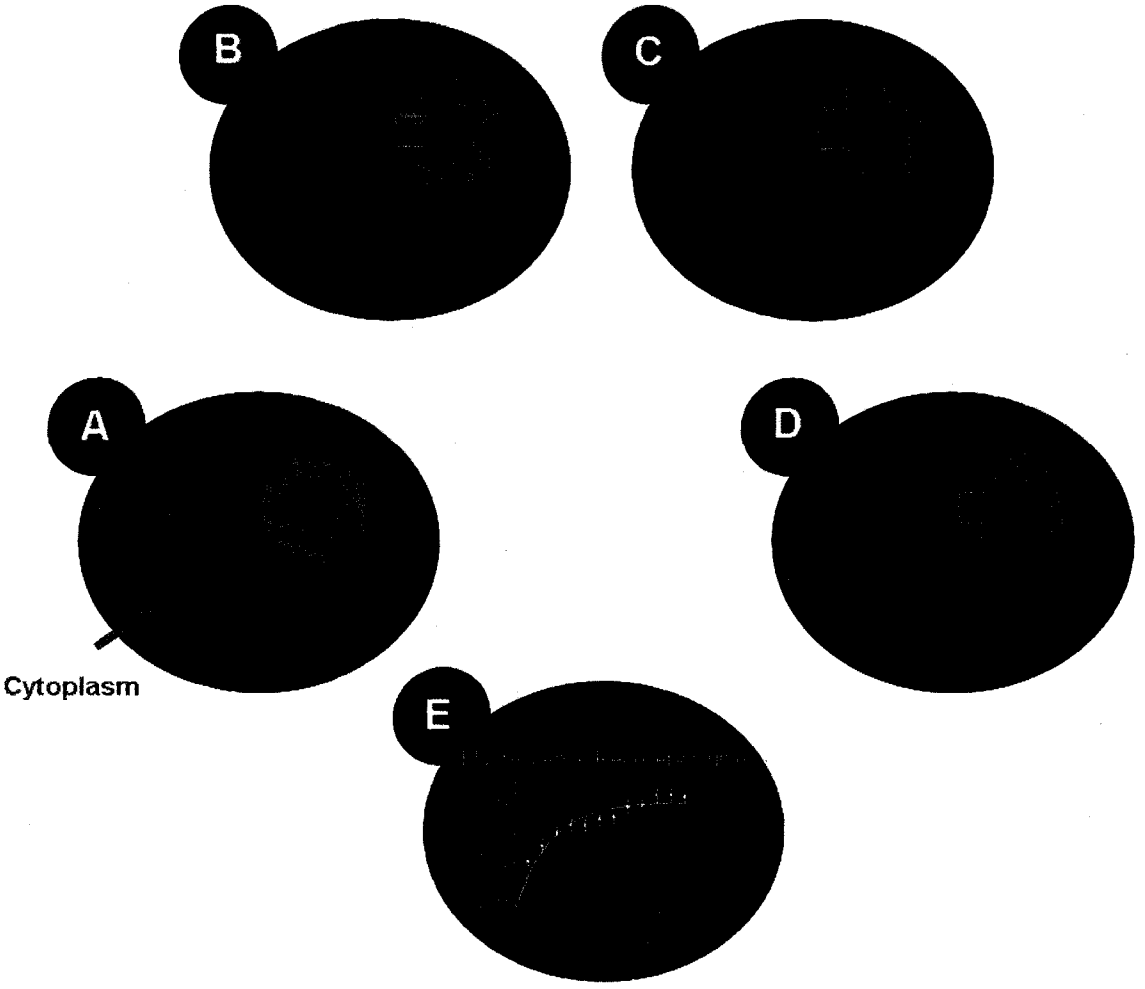

Figure 3. Fluorescence Recovery After Photobleaching. FRAP measures the kinetic diffusion rate of a protein. (**A**) The process starts with a strain that contains a protein of interest that is fluorescently tagged with GFP (or other fluorescent tag). A nuclear factor fused to GFP is used for this schematic. (**B**) A region of fluorescence is targeted for bleaching (red box). The region to be bleached is a relatively small area of the viewable signal. (**C**) The moment of bleaching is t_0 with respect to monitoring of the bleached population. (**D**) Time lapse microscopy is used to measure recovery over time. (**E**) The data are graphed relative to the pre-bleached intensity. The sample graph shown in (**E**) illustrates the kinetics of diffusion of a protein that recovers 50% of its final recovery (i.e. relative intensity) after ~300ms.

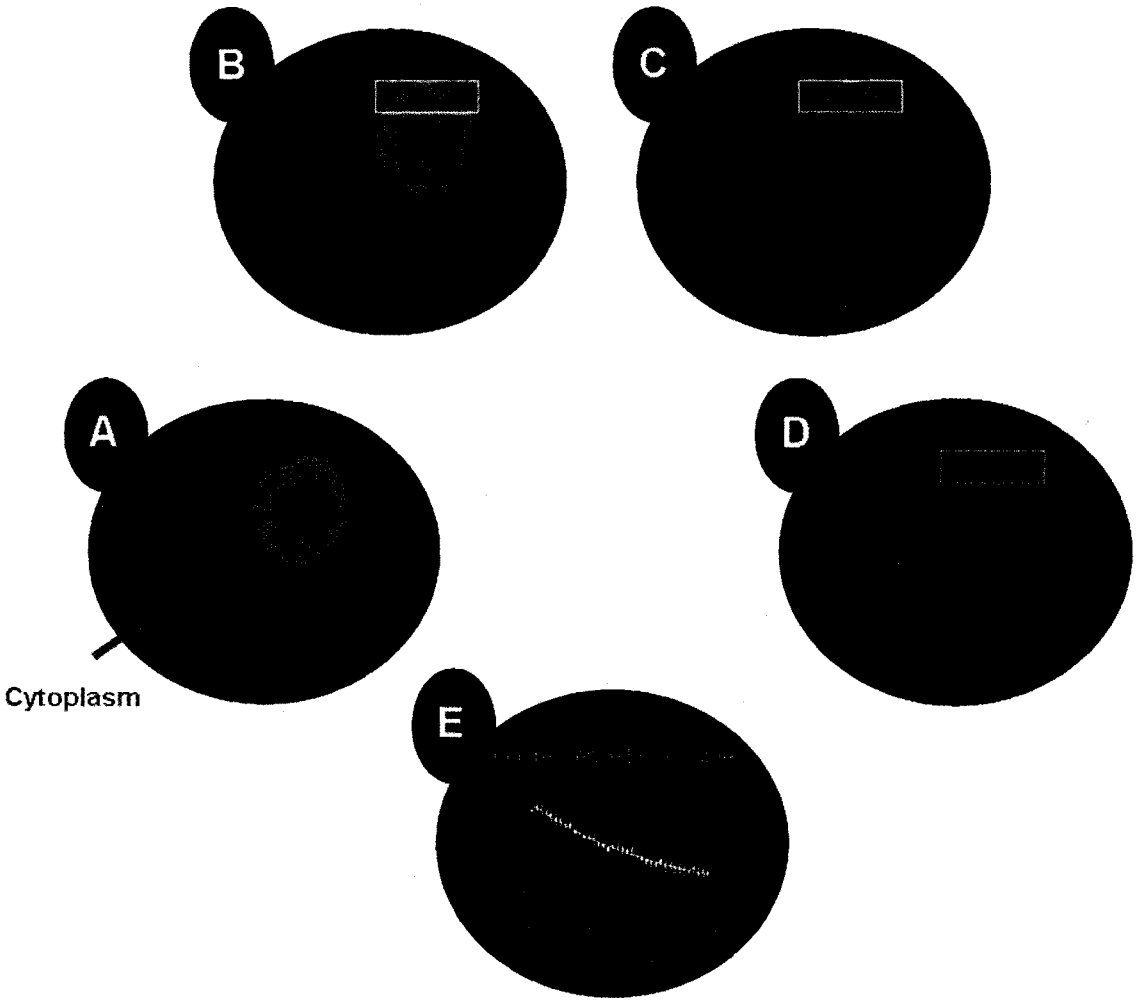

Figure 4. inverse Fluorescence Recovery After Photobleaching. iFRAP measures the kinetic dissociation rate of a protein. (**A**) The process starts with a strain that contains a protein of interest that is fluorescently tagged with GFP (or other fluorescent tag); a nuclear factor fused to GFP is used for this schematic. (**B**) The region of fluorescence is then divided into two smaller regions: a region to be bleached (red box) and a region to be subsequently monitored (yellow box). At least 60 to 80% of the viewable signal is targeted for bleaching. (**C**) The moment of bleaching is t_0 with respect to monitoring of the unbleached population. (**D**) Time lapse microscopy is used to measure signal degradation over time. (**E**) The data are graphed relative to the t_0 intensity. The sample graph shown in (**E**) illustrates the kinetics of dissociation of a protein that loses 50% of its fluorescence (i.e. relative intensity) after ~40 seconds.

In vivo gene tracking

Our understanding of chromatin organization and dynamics has progressed by a technique developed to track a single gene locus within a nucleus (Drubin *et al.* 2006).

By creating an array of binding sites within a host genome for the GFP fused bacterial Lac repressor, it is possible to observe a single locus *in vivo* (Figure 5). This technique has been utilized most recently to gain insight into gene movement within the nuclear lumen in the context of transcriptional regulation (reviewed in (Akhtar and Gasser 2007).

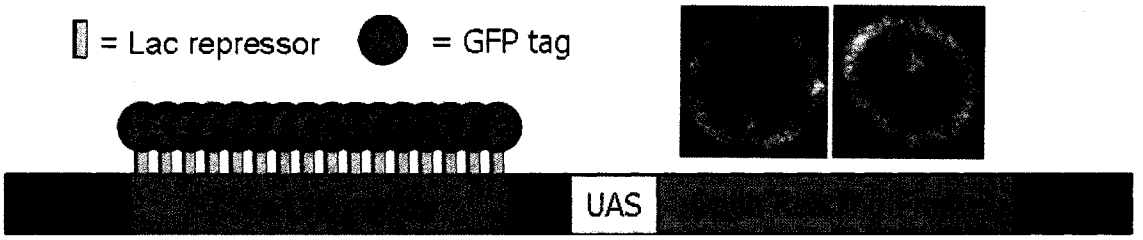

Figure 5. Gene tracking using LacI-GFP. An array containing 256 copies of the LacI DNA-binding sequence is inserted adjacent to the gene of interest. By expressing a plasmid borne LacI-GFP fusion protein it is possible to monitor the position of the tagged locus within the nucleus through the LacI binding array. Representative images on the right are of the *GAL1* locus. Nsp1-YFP marks the perinuclear compartment.

CHAPTER II

MATERIALS AND METHODS

Yeast Strains and Plasmids

Media preparation and basic yeast methods, such as lithium acetate transformation, were carried out according to standard procedures (Sherman 2002). Cells were grown in synthetic complete (SC) to which 2% glucose, 3% raffinose, 3% galactose or 3% pyruvate was supplemented as the carbon source; amino acids were dropped out as needed for plasmid selection. All cultures were grown at 30°C, unless otherwise noted; liquid cultures were incubated on a rotary wheel or shaking platform set to 200 rpm to maintain aeration. All assays were performed during the log phase growth.

S. cerevisiae strains and plasmids used in this study are listed in Table 1. The KB1017 strain was generated by 5-FOA selection of the PSY3354 strain to yield a *ura3-* strain (KB1016). To insert the GFP-RAS2 reporter gene in place of *GAL1*, GFP-RAS2-URA3 was amplified from the pWS270 plasmid (generous gift of Walter Schmidt) using oligonucleotides that contained 50 bp of homology to the sequences just upstream of the *GAL1* Start codon and downstream of the Stop codon. The amplified fragment was transformed into KB1016. *URA+* colonies were checked for proper integration by standard genomic DNA extraction and PCR.

To insert the lac_{op} array downstream of *GAL1* a 200 bp region of sequence that lies at +165 to +365 bp downstream of the *GAL1* Stop codon was amplified with oligonucletides that each included an SphI restriction site. The resulting PCR product was purifed, digested and ligated into the unique SphI site of pAFS59 to yield pAFS59-GAL1-int. Digestion with BsaAI was used to linearize pAFS59-*GAL1*-int within this

region, allowing integration of the entire plasmid into the yeast genome approximately 300 bp downstream of *GAL1*. Integrants were selected using SCD-LEU plates and integration of the plasmid was confirmed by standard genomic DNA extraction and PCR. The resulting strain is KB4462. To generate a Δ*gal4* version of this strain, the same exact method was used to insert the lac_{op} array downstream of *GAL1* in the *gal4*::KANMX4 strain from the yeast deletion set (Open Biosystems), to yield KB4363. This method was also used to introduce the lac_{op} array downstream of *GAL1* in the *rpb1-1* strain RS240 (generously provided by Dr. Michael Hampsey) to yield DB21. To generate a Δ*gal80* strain, the NATMX4 gene was amplified from the p4339 plasmid using oligonucleotides containing 50 bp of homology to the sequences just upstream of the *GAL80* Start codon and downstream of the Stop codon. The fragment was then transformed into KB4462 and NAT^R colonies isolated. Knock-out of *GAL80* was confirmed via PCR and the resulting strain is KB1015.

To insert the lac_{op} array upstream of *SUC2* a 300 bp region of sequence that lies at approximately -1500 to -1800 bp upstream of the *SUC2* Start codon was amplified with oligonucletides that each included KpnI and EcoRI restriction sites. This integration site was chosen because it was significantly far enough from the two Mig1 binding sites (which are located between -500 and -430 bp) in the *SUC2* promoter to avoid altering its regulation. The resulting PCR product was cloned into the TOPO-Blunt vector (Invitrogen) and then digested with KpnI+EcoRI and ligated into pAFS59 in a 3-fragment ligation (pAFS59 was disgested with EcoRI+BstEII and BstEII+KpnI). Digestion with NheI was used to linearize pAFS59-SUC2-int, allowing integration of the entire plasmid into the yeast genome approximately -1500 bp upstream of *SUC2*.

Integrants were selected using SCD-LEU plates and integration of the plasmid was confirmed by standard genomic DNA extraction and PCR. The resulting strain is KB38. To generate a Δ*mig1* and Δ*hxk2* versions of this strain, the same exact integration strategy was used to insert the lac_{op} array upstream of *SUC2* in the *mig1*::KANMX4 or *hxk2*::NATMX4 strain from the yeast deletion set (Open Biosystems; the *hxk2*::KANMX4 was switched to *hxk2*::NATMX4 using the EcoRI 'switcher' fragment from p4339), to yield KB39 and KB40, respectively.

Live Cell, Fluorescent Imaging

Mig1 localization

For Mig1 localization, cells expressing Mig1-GFP, from the yeast GFP clone collection (Invitrogen Life Technologies; see Table 1), and plasmid borne Rap1-CFP (nuclear marker; see Table 1), were imaged by using a Zeiss LSM 510 META confocal laser scanning microscope with a 63x Plan-Apochromat 1.4 NA Oil DIC objective lens. GFP was excited with the 488 nm laser and detected with the 505-530 BP filter. CFP was excited with the 458 nm laser and detected with the 475 LP filter. Pinholes were adjusted to obtain <1.8 μm optical slices. Cells were immobilized onto a 2% agarose pad supplemented with selective SC media containing either 2% glucose or 3% pyruvate for repressing and derepressing conditions, respectively.

SUC2 gene motion

For *in vivo* time course microscopy of *SUC2*, a Zeiss LSM510 META confocal microscope was used to visualize the nuclei of cells grown on selective SC media plates supplemented with either 2% glucose (repressed conditions) or 3% pyruvate (derepressed conditions). Wild type (*WT*; KB38) cells contained plasmid borne LacI-GFP (probe) and

Nsp1-YFP (peripheral marker), *HIS3* and *URA3* marked respectively. GFP and YFP were excited using the 488 nm and 514 nm lasers and detected with 505-530BP and 530LP filters, respectively. Imaging was done using an alpha Plan-Fluar 100x/1.45NA objective with a 1 μm depth of focus. Software zoom was utilized so that the resolution is such that 1 pixel = 0.04 μm. Each time lapse was performed over 4 minutes with an image taken every 60 seconds. Cells were immobilized onto a 2% agarose pad supplemented with selective SC media containing either 2% glucose or 3% pyruvate for repressing and derepressing conditions, respectively, and kept at 30°C during imaging by using a stage warmer.

GAL gene behavior and expression analysis in rpb1-1 cells

In vivo time course microscopy of the *GAL* genes was used in combination with Northern blot analysis to monitor gene position and expression during a transcriptional block. A temperature sensitive strain harboring the *rpb1-1* allele (which undergoes normal transcription at the 23°C permissive temperature, but no transcriptional initiation at the non-permissive temperature of 37°C; (Nonet *et al.* 1987) containing the lac_{op} array adjacent to the *GAL1* locus, a plasmid borne LacI-GFP (to visualize the gene spot) and Nsp1-YFP (nuclear marker; see Table 1) was used. Five 50 ml cultures, inoculated from the same stock, were grown at 23°C to an OD_{600} of 0.8 in selective SC media containing 3% raffinose. Each culture then underwent a specific treatment:

(A) Cells were grown at the permissive temperature of 23°C in 3% raffinose

(B) same as (A) and the cells were shifted to the non-permissive temperature of 37°C for 1 hour to shut off transcription of *rpb1-1*

(C) same as (B) and galactose was added to a final concentration of 2% while the cells were kept at the non-permissive temperature for 1 hour

(D) same as (C) with the cells being held at the non-permissive temperature for an additional 3 hours

(E) same as (D) with the cells being placed back at the permissive temperature of 23°C for 1 hour.

For each treatment, aliquots of the cultures were taken for confocal microscopy and to monitor expression. When viewing the cells on the LSM, permissive and non-permissive temperatures were maintained with the use of a heated stage (ambient temperature of the microscopy facility averages 20-21°C). Fluorescence detection of the gene (via lacI-GFP) and nuclear periphery (via Nsp1-YFP) were done as described for *SUC2* (see above). Cells were immobilized by using a 2% agarose pad containing SC media was supplemented with either 3% raffinose (uninduced conditions) or 3% galactose (induced conditions).

Expression was monitored by Northern blot analysis. Briefly, total RNA was isolated by using the previously published triazol method (Wang *et al.* 2004) and resolved on an agarose gel. The RNA was then transferred from the gel to a nytran membrane by using a Schleicher & Schuell TurboBlotter transfer system. The membrane was then probed with a ^{32}P-labelled oligonucleotide complementary to the *GAL1* mRNA or the highly stable *H1* mRNA (used here as a positive control) by using standard hybridization methods (Brown *et al.* 2004). The resulting ^{32}P-bound bands were imaged by using a phosphor screen and Typhoon Phosphorimager (GE Healthcare). Northern blot analyses presented here were contributed by Dr. David Buford.

SUC2 and GAL genes localization statistics

For *in vivo* localization statistics of *SUC2* and the *GAL* genes, a Zeiss LSM 510 confocal microscope was used to visualize cells grown in selective SC media supplemented with 2% glucose (repressed *SUC2*), 3% pyruvate (derepressed *SUC2*), 3% raffinose (uninduced *GAL1*), or 3% galactose (induced *GAL1*). *WT* and deletion mutants (KB38, KB39, KB40, KB4462, KB4363, and KB1015) contained the Lac array as described above as well as the corresponding plasmid-borne gene probe (LacI-GFP) and nuclear peripheral marker (Nsp1-YFP). Excitation and detection of GFP and YFP as well as cell immobilization were likewise done as described above. Imaging was done using an alpha Plan-Fluar 100x/1.45NA objective with a 1 μm depth of focus. For each condition at least 30 scans of independent fields, each containing at least 4 cells exhibiting normal nuclear morphology, a discernable nuclear ring and distinct gene spot, were captured. Subnuclear gene location was quantitated by measuring the distance from the center of the nucleus to the fluorescent gene spot and dividing that distance by the radius of the nucleus (determined as the distance from the nuclear center to the peak of Nsp1-YFP fluorescence). Genes that were measured to be equal to or greater than 67% of the distance of the nuclear radius were scored as perinuclear. Those measured to be less than 67% were scored as nucleoplasmic. Excel was used to record these measurements and calculate relevant error. At least 150 determinations were made for each condition.

Gal4 distribution in the nucleus

For *in vivo* Gal4-GFP distribution, a Zeiss LSM 510 confocal microscope was used to capture images of nuclei of cells grown in 3% galactose. *WT* cells (KEB3052) contained Nup49-tDimer2 and Nup60-tDimer2 (nuclear marker) along with plasmid

borne *WT* and variant forms of Gal4 tagged with GFP (see Table 1). Imaging was done using an alpha Plan-Fluar 100x/1.45NA objective with a 1 μm depth of focus. GFP and tDimer2 fusions were excited with the 488 nm and 543 nm lasers and detected with a 505-530BP and 585LP filters, respectively. Quantitation of peripheral Gal4 was measured by subtracting the GFP quantified within the inner 67% of the nucleus from the total nuclear GFP observed.

In vivo single cell analysis of GAL1 gene position and expression

For *in vivo* localization of the *GAL* genes in the fluorescent reporter strain containing *GFP-RAS2* in place of the *GAL1* coding region, a Zeiss LSM 510 confocal microscope was used to capture images of *WT* cells (KB3052 containing plasmid borne LacI-GFP (gene probe).

Cells were grown at 30°C in selective SC liquid media supplemented with 3% raffinose to an OD_{600} of 0.8. Localization of the uninduced *GAL* genes was scored as described above while the cells remained in 3% raffinose. To begin the induction, galactose was added to the growing culture to a final concentration of 2% and incubation at 30°C resumed. At 15, 30, 45, 60, 90 and 120 minutes post-induction, an aliquot of the culture was removed and 2 μl was deposited onto a lysine coated glass slide. For each time point, images of cells were captured within 5 minutes as described above (see *SUC2* and *GAL* localization statistics). In order to collect enough cells for scoring, this experiment was repeated 3 times. This experiment was also repeated with the time points of 30, 35, 40 and 45 minutes post galactose induction. For this reduced time, images for each time point were captured within 2.5 minutes. This additional analysis was repeated 3 times.

Scoring of the gene localization was done as described above (see *SUC2* and *GAL* localization statistics). *GFP-RAS2* expression was measured by observing a cross section of the cell that extended from one edge of the cell periphery to the other. Fluorescence levels were exported to Excel for analysis with a file coding system in order to correlate the gene location with expression of the reporter. Cells were determined to be actively expressing *GFP-RAS2* if the level of GFP fluorescence intensity at the cell cortex (the well-established location of Ras2, reviewd in (Santangelo 2006)) was equal to at least twice the ambient background levels. Cells were maintained at 30°C using a stage warmer.

GFP Fluorescence Recovery After Photobleaching (FRAP)

FRAP was performed on cells (BY4742) containing plasmid borne native Gal4 fused with GFP (YEpHIS-Gal4-GFP), Gal4 derivatives or chromosomally expressed Htb2-GFP from the yeast GFP clone library (see Table 1).

Cells were grown in 3% raffinose at 30°C to an OD_{600} of 0.8. For inducing conditions, galactose was added to the culture to a final concentration of 2% and incubation resumed for an additional 2 hours before assaying. FRAP was done with a Zeiss LSM 510 confocal microscope. Assayed cells were placed on a lysine coated slide and kept at 30°C with a stage warmer. For this experiment, GFP was excited and photobleached using the 488 nm laser (see details below) and subsequent recovery was observed with the 505-530BP filter. Imaging was done using an alpha Plan-Fluar 100x/1.45NA objective with a 1 μm depth of focus and the software zoom set to 10.

Live cells expressing the target nuclear protein tagged with GFP were first subjected to a single regional bleaching event of .15 - .2 μm squared area of the

fluorescent population with the 488 nm laser set to 100%. Subsequent images were taken every 250 ms up to 3 seconds. Regions of interest (ROI) were recorded from the region left unbleached (Reference ROI), the bleached region (FRAP ROI), both bleached and unbleached region (Whole cell ROI) and a region outside of the nucleus (Base ROI). Each fluorescence intensity of each ROI over the course of the experiment was recorded in Excel for calculating the recovery curve. The normalized recovery curve was calculated as follows:

FRAP ROI: $I_{frap}(t)$

Reference ROI: $I_{ref}(t)$

Base ROI: $I_{base}(t)$

Whole Cell ROI: $I_{whole}(t)$

$$I_{frap-norm}(t) = \frac{I_{whole-pre}}{I_{whole}(t) - I_{base}(t)} \cdot \frac{I_{frap}(t) - I_{base}(t)}{I_{frap-pre}}$$

It should be noted that the reference ROI should not show a significant drop in fluorescence as a result of the bleach event.

Recovery curves were imported into GraphPad Prism 4 where they were fit to a single exponential association equation for the purposes of determining the $t_{1/2}$ of recovery. For each condition, at least 5 FRAP experiments were performed and the average curve is reported.

GFP inverse Fluorescence Recovery After Photobleaching (iFRAP)

Cells assayed by iFRAP were handled identically as for FRAP except proteins tagged with GFP that were not under the GAL regulatory system were grown in either 2% glucose or 3% pyruvate (*SSN6-GFP*). As in the FRAP analysis, Gal4-GFP was expressed from a plasmid; all other GFP fusions examined are from the yeast GFP

collection (see Table 1). Imaging done for iFRAP was likewise done with the same equipment setup and slide preparation as described for FRAP (see above).

Live cells expressing the target nuclear protein tagged with GFP were first subjected to a single bleaching event of 65-80% of the fluorescent population with the 488 nm laser set to 100%. Subsequent images were taken on a timescale dependent on the stability of the signal observed: every 0.5, 1.0 or 1.5 seconds. At least 20 images were captured for each condition. Regions of interest (ROI) were recorded from the region left unbleached (iFRAP ROI), the bleached region (Reference ROI) and a region outside of the nucleus (Base ROI). It should be noted that the reference ROI was taken as the inverse of the FRAP reference ROI. The fluorescence intensity of each ROI over the course of the experiment was recorded in Excel for calculating the fluorescence loss curve. In order to calculate the normalized curve:

iFRAP ROI: $I_{ifrap}(t)$

Reference ROI: $I_{ref}(t)$

Base ROI: $I_{base}(t)$

$$I_{ifrap\text{-}norm}(t) = \frac{(I_{ifrap}(t) - I_{base}(t)) - (I_{ref}(t) - I_{base}(t))}{(I_{ifrap\text{-}post} - I_{base\text{-}post}) - (I_{ref\text{-}post} - I_{base\text{-}post})}$$

It should be noted that acquisition bleaching for each condition averaged 0.03% per scan.

Fluorescence loss curves were imported into GraphPad Prism 4 where they were fit to a single exponential dissociation equation for the purposes of determining the $t_{1/2}$ of recovery. For each condition, at least 3 iFRAP experiments were performed.

Gal4 Variant Cloning

Gal4 variants were produced by replacement of a target domain(s) within the protein with the SV40 nuclear localization sequence (NLS). All derivatives were cloned with a plasmid containing native Gal4, fused with GFP, to be recombined with a linear

fragment comprised of the SV40 NLS flanked by 50 bp of homology to the 50 bp immediately adjacent to the target domain(s) to be replaced. Homologous recombination cloning was done in yeast cells that were deleted for *GAL4* to prevent possible chromosomal integration of the desired Gal4 variant.

Each linear fragment was created by PCR of the SV40 NLS sequence from the plasmid pJK202. The 5' oligo contained 50 bp homology to the 5' sequence adjacent to the target domain to be replaced and 18 bp of homology to the SV40 NLS sequence. The 3' oligo contained 50 bp homology to the 50 bp adjacent to the 3' end of the target domain and again 18 bp homology into the 3' end of the SV40 NLS sequence. Regions of Gal4 replaced by the NLS sequence were: residues 2-50 (DNA-binding domain; ΔDBD), residues 2-147 (both DNA-binding domain and the dimerization domain; AD), residues 50-97 (dimerization domain; ΔDD), residues 768-881 (primary activation domain; ΔAD1) and residues 147-881 (both primary and secondary activation domains; ΔAD2).

Cells were co-transformed, with linearized YEpHIS-Gal4-GFP (within the domain to be replaced) and accompanying PCR fragment (see above). Transformed cells were then plated onto solid SC media containing 2% glucose selecting for *HIS3* and grown for 48 hours at 30°C. Candidate colonies that grew were inoculated into 5mL selective SC media (a maximum of 6 were tested at a time) and grown at 30°C to an OD_{600} of 0.8. Standard yeast mini-lysate DNA extracts were done for each of the 6 cultures to extract the plasmid DNA. Removal of each targeted region was confirmed by using standard restriction digests. Confirmed plasmid constructs (see Table 1) were transformed into DH5α *E. coli* for amplification and subsequent purification by using a

standard alkaline lysis method with phenol/chloroform extraction (Engebrecht *et al.* 2001).

Chromatin Immunoprecipitation (ChIP)

ChIP was done as described below (Sarma 2007). For *SUC2* regulatory system studies, 50 ml TAP tagged strains (see Table 1) were grown in YEP supplemented with either 2% Glucose (Repressed) or 3% Pyruvate (derepressed) at 30°C. The ChIP assays presented here were provided by Dr. Nayan Sarma and were performed as described in Sarma 2007 (Sarma 2007).

Cell Fractionation and Quantitative Fluorescent Protein Detection (QFPD)

Cell Fractionation

Three liters of liquid SC media supplemented with a specific carbon source (i.e. 2% glucose, 3% pyruvate, 3% raffinose or 3% galactose) were inoculated with a yeast strain expressing either a tagged (i.e. GFP or TAP) or *WT* (in the case of a native antibody being used) target protein (see Table 1). Cultures were harvested at an OD_{600} of 0.8.

Cells were collected by centrifugation at 8,000 x g for 5 minutes at 4°C. After centrifugation, the supernatant was decanted and the cell pellets were thoroughly washed with the following solutions: 50 mL of cold Type I sterile water, 20 mL Tris-DTT (1 M Tris, 0.1M DTT), 20 mL of cold Type I sterile water, and finally, 20 mL of 1.1 M Sorbitol. For each washing step, the cell pellet was resuspended in the solution and then collected by centrifugation at 2,000 x g for 5 minutes at 4°C. Following each wash the supernatants were decanted and discarded.

For spheroplast digestion, cell pellets were resuspended with 12.5 mL of 1.1 M Sorbitol and transferred to a sterile 125 mL flask. To each flask 375 µl of Zymolyase solution (10% Zymolyase, 1.1 M Sorbitol), 500 µl glusulase and 62.5 µl of 1 M DTT was added. All flasks were incubated in a rotating 30°C water bath on a slow setting for 3 hours. Every 15 minutes, the flasks were swirled manually to help keep cells suspended in solution. When the 3 hours of digestion was complete, spheroplasts were confirmed by viewing on a light microscope.

The digested cells were then transferred to Nalgene-30 tubes and collected by centrifugation at 2,000 x g for 5 minutes at 4°C. Each supernatant was carefully removed and discarded and the pellet resuspended in 10 mL of 1.1 M Sorbitol. Next, the samples were carefully poured into Nalgene-30 tubes containing 10 mL Ficoll-Sorbitol (12% Ficoll-400, 1.1 M Sorbitol). The samples were centrifuged at 10,000 x g for 15 minutes at 4°C. Once the centrifugation was complete, the supernatant was carefully discarded from each sample and the pellet was rinsed one time with 10 mL of 1.1 M Sorbitol to remove the remaining Ficoll.

To each tube, 15 mL of the spheroplast lysis solution (8% Polyvinylpyrrolidone [PVP], .25% TritonX-100, 5 mM DTT, 1X PI cocktail 1 mM PMSF) was added and placed on ice. In a cold room (4°C) each pellet was resuspended by sonication using a Polytron (Polytron Devices) set to 3 for 1 minute then placed on ice for 1 minute. Spheroplasts were then ruptured by sonication using the Polytron set to 3.5 for 1 min. Each sample was then underlayed with 10 mL of 0.6 M Sucrose, 8% PVP, 1 mM PMSF, 1X PI solution by slowly pipetting directly into the bottom of the tube. The tubes were then centrifuged at 16,000 x g for 20 minutes at 4°C. After centrifugation 3 mL of the

supernatant (cytosolic samples) were transferred into sterile 15 mL tubes and stored at -80°C.

The pellets (nuclei samples) were then resuspended in 2 mL of 2.1 M Sucrose/ PVP. Each of the nuclei samples were gently transferred onto previously prepared sucrose gradient columns. Sucrose gradients were made from 2.3 M, 2.1 M or 2.01 M sucrose solutions containing 8% PVP, protease inhibitor (PI; 0.005 mM Pepstatin A) and 1 mM PhenolMethylSulfonylFluoride (PMSF) respectively. The gradients were formed by slowly layering 1 mL of each solution in Beckman Polyallomer tubes, starting with the most dense layer (2.3 M Sucrose/PVP) and ending with the least dense layer (2.01 M Sucrose/PVP).

The columns were then placed within a SW-55 swinging bucket rotor (Beckman) and ultra-centrifugation was done at 29,300 rpm for 8 hours under 200 μm vacuum at 4°C. Tubes were placed on ice after completion of the spin. The top clear zone and the cloudy interphase fraction were pipetted off and discarded. The beige-colored region containing nuclei was transferred to 5 mL Falcon tubes and placed on ice. The pellet was discarded. Next, 1 mL of each nuclei sample was transferred to Beckman 30 mL TY50 2Ti tubes and overlayed with 8% PVP solution to the neck of the tube (~21 mL). The remaining nuclei samples were stored in the 5 mL Falcon tubes at -80°C.

The Beckman tubes underwent ultra-centrifugation in the 70TI rotor at 48,000 rpm for 1 hour under 200 μm vacuum at 4°C. After centrifugation, the supernatant was removed from each sample by gentle inversion and dabbing on a Kim-Wipe. The pellet was then resuspended in 500 μl of cold nuclear lysis solution (1 M Bis-Tris HCl, pH 6.5, 1 mM PMSF, .005 mM PI, and .002% DNAseI) and mixed by vortexing in 30 second

intervals before letting sit at room temperature for 5 minutes. 500 ml of Sucrose/Nycodenz solution was added to sterile 1.5 mL microfuge tubes and the resuspended pellets were subsequently added and mixed by vortexing. The tubes were then centrifuged at 4,350 x g for 6 minutes at 4°C. After the spin, the supernatant (nuclear envelope sample) was then added to sterile Beckman Polyallomer tubes followed by the addition of 2 mL of Sucrose/Nycodenz (20% Nycodenz, 2.3 M Sucrose, 10 mM Bis-Tris HCl, pH 6.5, 100 mM $MgCl_2$). Covering the top of the tubes with parafilm each tube was vortexed for mixing. After removing the parafilm the samples were overlayed first with 1 mL of 2.25 M Sucrose, 100 mM Bis-Tris HCl, pH 6.5, and 0.1 mM $MgCl_2$ and then 1 mL of 1.5M Sucrose, 100mM Bis-Tris HCl, pH 6.5, and 0.1mM $MgCl_2$. The tubes were placed within the SW-55 rotor (Beckman) and ultra-centrifuged at 41,000 rpm for 24 hours under 200 μm vacuum at 4°C.

After centrifugation the clear top regions were discarded from the gradient. The beige region, containing the nuclear envelope sample, was pipetted off and transferred to 30 mL Nalgene-30 tubes and placed on ice. The nuclei and cytosolic samples were then thawed on ice and also transferred to 30 mL Nalgene-30 tubes on ice. To each tube, 9 mL of cold Methanol was added and all tubes were placed at -20°C for 1 hour. The samples were then centrifuged at 10,000 rpm for 10 minutes at 4°C. After discarding the supernatant, the pellets were suspended in 300 μl of Buffer C (10% Glycerol, 0.3 M ammonia sulfate, 0.5 M Tris, pH 8.0, 10 mM $MgCl_2$, 10 mM EDTA) and placed on ice. Finally, all resuspended samples were transferred to microfuge tubes and centrifuged at 10,000 rpm for 5 minutes at 4°C to pellet debris.

All samples were assayed for protein content using a Bradford Assay using 0, 1, 2, 4, 8 and 16 μg of BSA in 1 mL of Bradford solution (1:5 dilution of the Bradford Reagent [Biorad] in Type I sterile water) to create a standard curve. Protein estimations were measured using 5 ml of each cytosolic, nuclei and nuclear envelope samples with 1 mL of Bradford solution.

Quantitative Fluorescent Protein Detection

Using a 96-well plate, 0, 2, 4, 8 and 16 mg of each fraction (i.e. cytosolic, nuclei and nuclear envelope) were loaded into horizontal adjacent wells. Volume in the wells was standardized by adding Buffer C (200 mM Tris, pH 8, 10 mM $MgCl_2$, 10 mM EDTA, 300 mM $(NH_4)_2SO_4$, 10% glycerol) to samples where necessary. Each well was then mixed gently by pipetting and the plate was placed on the phosphorimager (GE Healthcare) for scanning. GFP tagged protein was detected by the phosphorimager by exciting the fluorescent protein with the blue2-488 nm laser and detected with a 526SP filter. The sensitivity was set to high and the photo-multiplier tube 800 V. Pixel resolution was set to 200 μm and the focal plane was adjusted to +3 mm above the platen. Densitometry of each well was calculated using ImageQuant software (GE Healthcare). The background fluorescence was calculated from the 0 μg wells and was subtracted from each other well in the corresponding set. Total fluorescence for each set was then added for each fraction that was isolated. The nucleoplasmic signal was normalized by subtracting the nuclear envelope intensity. The QFPD and Co-fractionation assays presented here were contributed by Dr. David Buford.

Co-immunoprecipitation and Western blots

For immunoprecipitation of Mig1, a GFP tagged Mig1 strain with appropriate lexA-tagged plasmids (see Table 1) was grown in 25 ml SC + 2% glucose. In case of immunoprecipitation of Gal4, cells with appropriate lexA-tagged plasmids were grown in SC supplemented with either 3% galactose (induced) or 3% raffinose (uninduced). The co-immunoprecipitation and western blot assays presented here were contributed by Dr. Nayan Sarma and were performed as described in Sarma 2007 (Sarma 2007).

Table 1. Yeast strains and plasmids

Strain	Genotype	Reference
BY263	MATa, *ade2-107, his3Δ200, leu2-Δ1, trp1Δ63, ura3-52, lys2-801*	(Measday *et al.* 1994)
BY4742	MATα, *his3Δ1, leu2Δ0, lys2Δ0, ura3Δ0*	(Winzeler *et al.* 1999)
DB21	Same as RS420 but *GAL1-lac$_{op}$* x 256 (*LEU2*)	This work
KB1015	Same as KB4462 and *gal80*:: NATMX4	This work
KB1016	Same as PSY3364 but *ura3-*	This work
KB1017	Same as PSY3364 and *gal1*::GFP-*RAS2*	This work
KB3	Same as BY263 but *lac$_{op}$* x 256 (*LEU2*)-*SUC2*	(Sarma *et al.* 2007)
KB39	Same as BY4742 but *mig1*::KANMX4, *lac$_{op}$* x 256 (*LEU2*)-*SUC2*	(Sarma *et al.* 2007)
KB40	Same as BY4742 but *hxk2*::NATMX4, *lac$_{op}$* x 256 (*LEU2*)-*SUC2*	(Sarma *et al.* 2007)
KB4363	Same as BY4742 but *gal4*::KANMX4 and *GAL1-lac$_{op}$* x 256 (*LEU2*)	This work
KB4462	Same as BY4742 and *GAL1-lac$_{op}$* x 256 (*LEU2*)	This work
KEB3052	Same as KB1017 but *his3Δ* (for this strain lacI-GFP must be plasmid-borne in order to visualize the *GAL1* gene)	This work
PSY3364	MATa, *ade2-1, trp1-1, can1-100, NUP49*-tdimer2-*URA3*, *NUP60*-tdimer2-KANMX4, *lac$_{op}$*x256 intergenic to *GAL7* and *GAL10, his3*::GFP-*lacI-HIS3*	(Drubin *et al.* 2006)
RS420	MATa *ura3-53, his4, trp1, leu2-3,112, rpb1-1*	(Nonet *et al.* 1987)
Esc1-GFP	MATa *leu2Δ0, met15Δ0, ura3Δ0*, Esc1-GFP-*HIS3*	(Huh *et al.* 2003)
Fhl1-GFP	MATa *leu2Δ0, met15Δ0, ura3Δ0*, Fhl1-GFP-*HIS3*	(Huh *et al.* 2003)
Gcr1-GFP	MATa *leu2Δ0, met15Δ0, ura3Δ0*, Gcr1-GFP-*HIS3*	(Huh *et al.* 2003)
Hda1-GFP	MATa *leu2Δ0, met15Δ0, ura3Δ0*, Hda1-GFP-*HIS3*	(Huh *et al.* 2003)

Htb2-GFP	MATa *leu2Δ0*, *met15Δ0*, *ura3Δ0*, Htb2-GFP-*HIS3*	(Huh *et al.* 2003)
Med1-GFP	MATa *leu2Δ0*, *met15Δ0*, *ura3Δ0*, Med1-GFP-*HIS3*	(Huh *et al.* 2003)
Mig1-GFP	MATa *leu2Δ0*, *met15Δ0*, *ura3Δ0*, Mig1-GFP-*HIS3*	(Huh *et al.* 2003)
Nup133-GFP	MATa *leu2Δ0*, *met15Δ0*, *ura3Δ0*, Nup133-GFP-*HIS3*	(Huh *et al.* 2003)
Nup60-GFP	MATa *leu2Δ0*, *met15Δ0*, *ura3Δ0*, Nup60-GFP-*HIS3*	(Huh *et al.* 2003)
Nup84-GFP	MATa *leu2Δ0*, *met15Δ0*, *ura3Δ0*, Nup84-GFP-*HIS3*	(Huh *et al.* 2003)
Pom34-GFP	MATa *leu2Δ0*, *met15Δ0*, *ura3Δ0*, Pom34-GFP-*HIS3*	(Huh *et al.* 2003)
Rap1-GFP	MATa *leu2Δ0*, *met15Δ0*, *ura3Δ0*, Rap1-GFP-*HIS3*	(Huh *et al.* 2003)
Rpb1-GFP	MATa *leu2Δ0*, *met15Δ0*, *ura3Δ0*, Rpb1-GFP-*HIS3*	(Huh *et al.* 2003)
Sac3-GFP	MATa *leu2Δ0*, *met15Δ0*, *ura3Δ0*, Sac3-GFP-*HIS3*	(Huh *et al.* 2003)
Sgf73-GFP	MATa *leu2Δ0*, *met15Δ0*, *ura3Δ0*, Sgf73-GFP-*HIS3*	(Huh *et al.* 2003)
Ssn6-GFP	MATa *leu2Δ0*, *met15Δ0*, *ura3Δ0*, Ssn6-GFP-*HIS3*	(Huh *et al.* 2003)
Ste12-GFP	MATa *leu2Δ0*, *met15Δ0*, *ura3Δ0*, Ste12-GFP-*HIS3*	(Huh *et al.* 2003)
Swi4-GFP	MATa *leu2Δ0*, *met15Δ0*, *ura3Δ0*, Swi4-GFP-*HIS3*	(Huh *et al.* 2003)
Gal11-TAP	MATa *leu2Δ0*, *met15Δ0*, *ura3Δ0*, Gal11-TAP-*HIS3*	(Ghaemmaghami *et al.* 2003)
Med1-TAP	MATa *leu2Δ0*, *met15Δ0*, *ura3Δ0*, Med1-TAP-*HIS3*	(Ghaemmaghami *et al.* 2003)
Mig1-TAP	MATa *leu2Δ0*, *met15Δ0*, *ura3Δ0*, Mig1-TAP-*HIS3*	(Ghaemmaghami *et al.* 2003)
Nop1-TAP	MATa *leu2Δ0*, *met15Δ0*, *ura3Δ0*, Nop1-TAP-*HIS3*	(Ghaemmaghami *et al.* 2003)
Nup133-TAP	MATa *leu2Δ0*, *met15Δ0*, *ura3Δ0*, Nup133-TAP-*HIS3*	(Ghaemmaghami *et al.* 2003)
Nup145-TAP	MATa *leu2Δ0*, *met15Δ0*, *ura3Δ0*, Nup145-TAP-*HIS3*	(Ghaemmaghami *et al.* 2003)
Nup53-TAP	MATa *leu2Δ0*, *met15Δ0*, *ura3Δ0*, Nup53-TAP-*HIS3*	(Ghaemmaghami *et al.* 2003)
Pom152-TAP	MATa *leu2Δ0*, *met15Δ0*, *ura3Δ0*, Pom152-TAP-*HIS3*	(Ghaemmaghami *et al.* 2003)
Rpb1-TAP	MATa *leu2Δ0*, *met15Δ0*, *ura3Δ0*, Rpb1-TAP-*HIS3*	(Ghaemmaghami *et al.* 2003)
Rpb7-TAP	MATa *leu2Δ0*, *met15Δ0*, *ura3Δ0*, Rpb7-TAP-*HIS3*	(Ghaemmaghami *et al.* 2003)
Ssn6-TAP	MATa *leu2Δ0*, *met15Δ0*, *ura3Δ0*, Ssn6-TAP-*HIS3*	(Ghaemmaghami *et al.* 2003)
Ssn8-TAP	MATa *leu2Δ0*, *met15Δ0*, *ura3Δ0*, Ssn81-TAP-*HIS3*	(Ghaemmaghami *et al.* 2003)
Taf14-TAP	MATa *leu2Δ0*, *met15Δ0*, *ura3Δ0*, Taf14-TAP-*HIS3*	(Ghaemmaghami *et al.* 2003)
Tbp1-TAP	MATa *leu2Δ0*, *met15Δ0*, *ura3Δ0*, Tbp1-TAP-*HIS3*	(Ghaemmaghami *et al.* 2003)

Plasmid	Characteristics	Reference
P4339	pCRII-TOPO (Invitrogen) – natMX4	(Tong *et al.* 2001)
pAFS59	pMB1 ori, Amp^r, *LEU2*, 256 Lac operator array	(Straight *et al.* 1996)
pAFS59-GAL1-int	Same as pAFS59 plus 200bp of *GAL1* flanking sequence (see text for details)	This work
pAFS59-SUC2-int	Same as pAFS59 plus 300bp of *SUC2* flanking sequence (see text for details)	This work
pHKB	CEN/ARS ori, *HIS3*, Amp^r, pMB1 ori	This work
pHKB-Rap1-CFP	Derivative of pHKB encoding P_{RAP1}Rap1-CFP	(Sarma *et al.* 2007)
pHKB-LacI-GFP	Derivative of pHKB encoding P_{RAP1}-LacI-GFP	(Sarma *et al.* 2007)
pHKB-LacI-GFP-GAL1	Derivative of pHKB encoding P_{RAP1}-LacI-GFP and P_{GAL1}*GAL1*	This work
pJK202	2-μ ori, *HIS3*, Amp^r, P_{ADH1}-lexA-NLS	(Origene)
pWS270	*CEN URA3* P_{GAL}-*GFP-RAS2*	(Manandhar *et al.* 2007)
YCp50	CEN/ARS ori, *URA3*, Amp^r, pMB1 ori	(Rose *et al.* 1987)
YCp50-Nsp1-YFP	Derivative of YCp50 encoding P_{NSP1}-*NSP1*-YFP	This work
YEpHIS	2-μ ori, *HIS3*, Amp^r, pMB1 ori	This work
YEpHIS-Gal4^{AD}-GFP	Same as YEpHIS plus P_{GAL4}-*GAL4*$^{\Delta 2\text{-}147}$-GFP	This work
YEpHIS-Gal4$^{\Delta AD1}$-GFP	Same as YEpHIS plus P_{GAL4}-*GAL4*$^{\Delta 768\text{-}881}$-GFP	This work
YEpHIS-Gal4$^{\Delta AD2}$-GFP	Same as YEpHIS plus P_{GAL4}-*GAL4*$^{\Delta 147\text{-}881}$-GFP	This work
YEpHIS-Gal4$^{\Delta DBD}$-GFP	Same as YEpHIS plus P_{GAL4}-*GAL4*$^{\Delta 2\text{-}50}$-GFP	This work
YEpHIS-Gal4$^{\Delta DD}$-GFP	Same as YEpHIS plus P_{GAL4}-*GAL4*$^{\Delta 50\text{-}97}$-GFP	This work
YEpHIS-Gal4-GFP	Same as YEpHIS plus P_{GAL4}-*GAL4*-GFP	This work
YEpTRP-Nup84-LexA	2-μ ori, *TRP1*, Amp^r Nup84-lexA	(Sarma *et al.* 2007)

CHAPTER III

iFRAP ANALYSIS OF YEAST NUCLEAR FACTORS

Our lab has reported that the NPC can be a site of transcriptional activation (Menon *et al.* 2005). One possible explanation is that activation occurs at bona fide NPCs but an alternative possibility is that components of the nuclear pores activate gene expression when dissociated from NPCs. If this were the case we might observe that a portion of NPC components would have a relatively rapid dissociation rate, as determined by photobleaching techniques. Traditional methods of elucidating protein-protein interactions are performed *in vitro*. An intrinsic challenge when using this approach is how to relate an *in vitro* result to an *in vivo* process. Many proteins are compartmentalized as a feature of their function; for example the repressor Mig1 is evicted from the nucleus in the absence of glucose repression (Sarma *et al.* 2007). A consequence of *in vitro* techniques is the disruption of cellular compartments. Because of this drawback, I chose to use inverse fluorescence recovery after photobleaching (iFRAP). This photo-bleaching technique (see Background) measures the dissociation of a GFP-tagged protein from a target complex. Figure 6 shows representative individual iFRAP experiments for relatively stable NPC component Pom34 and highly mobile Fhl1.

Nuclear Pore Complex Components Form Stable Structures

The NPC facilitates the transfer of material in and out of the nucleus. Similar to a study on human nucleoporins (Rabut *et al.* 2004), factors that constitute the membrane embedded NPC exhibited a relatively slow dissociation rate, which can also be described

as structural residence time ($t_{1/2}$ of fluorescence loss), as compared to the other nuclear

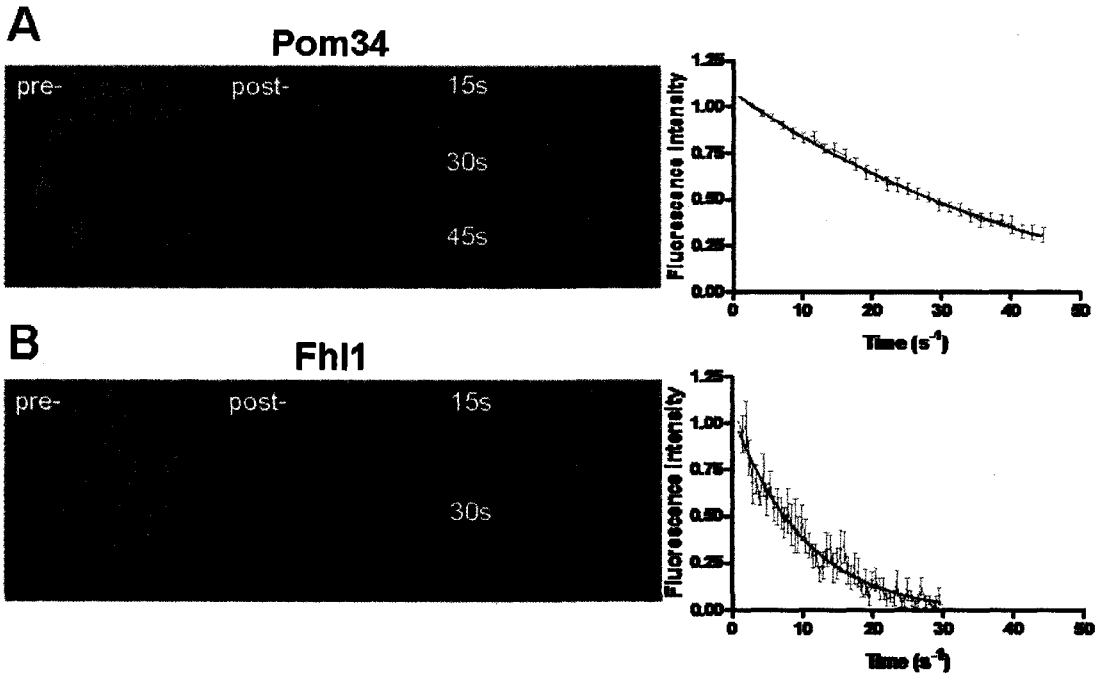

Figure 6. iFRAP can distinguish slow- vs. fast-dissociating nuclear factors in yeast. iFRAP analysis of Pom34-GFP, an integral nuclear membrane protein and known structural constituent of the nuclear pore complex, and Fhl1-GFP, a transcription factor involved in activation of the ribosomal protein genes, was done as described in Figure 4. GFP was excited with a 488nm laser. The resulting fluorescent emissions were detected by using a 505-530BP filter. The loss of fluorescence from Pom34-GFP (**A**) and Fhl1-GFP (**B**) was monitored over 45 and 30 seconds, respectively. The 'pre' frame above represents the total GFP signal prior to regional bleaching. The 'post' frame represents the scan immediately following the bleach event. Three replicate iFRAP analysis were done for each protein. The resulting averages were graphed (right panel). Pom34 shows a significantly slower dissociation rate (t1/2 = 40s) than Fhl1 (t1/2 = 10s).

factors tested (Table 2). An exception to this general observation was the nuclear exportin Sac3 with a residence time of 20s. This mobility difference was most notable in the fluorescence decay curve, in which the Sac3 curve separated from the other four curves (Figure 7A). Sac3 is reported to associate with Nup1 and assists in mRNA export across the nuclear membrane (Lei *et al.* 2003). The remaining NPC factors Nup60, Nup84,

Nup133 and Pom34 are constituents of the pore structure and resided within the complex at least twice as long as Sac3 (Table 2).

Table 2: Dissociation kinetics of nuclear proteins

Nuclear Factor		$k_{(off)}(s^{-1})^a$ 10^{-2}	Residence Time (s)[b]	Biological Function
Nuclear Pore Factors				
Nup84		1.60 ± 0.21	62.50	Component of Nup84 subcomplex
Nup133		1.90 ± 0.14	52.63	Component of Nup84 subcomplex
Nup60		1.90 ± 0.19	52.63	NPC structural component
Pom34		2.50 ± 0.14	40.00	NPC structural component
Sac3		5.00 ± 0.45	20.00	Nuclear export factor
Chromosomal Factors				
Htb2		2.30 ± 0.44	43.48	Core histone component
Sgf73		10.00 ± 0.49	10.00	SAGA recruitment factor
Hda1		11.00 ± 1.60	9.09	Histone deacetylase
Mediator / RNA Polymerase II				
Rpb1		2.20 ± 0.09	45.45	Large subunit of RNA pol II
Med1		18.00 ± 0.75	5.56	Mediator subunit
Transcription Factors				
Rap1[c]		2.00 ± 0.47	50.00	RP / Glucose activator
Gcr1		2.10 ± 1.20	47.62	RP / Glucose activator
Esc1		2.30 ± 0.30	43.48	Telomere silencing factor
Swi4		8.70 ± 0.44	11.49	G1 specific activator
Gal4	Raffinose	9.30 ± 0.93	10.75	Galactose activator
	Galactose	3.20 ± 0.56	31.25	
Fhl1		9.70 ± 1.10	10.31	RP activator
Ste12		11.00 ± 0.89	9.09	Mating activator
Ssn6	Dextrose	10.00 ± 0.65	10.00	Glucose repressor
	Pyruvate	14.00 ± 1.20	7.14	
Mig1		17.00 ± 2.40	5.88	Glucose repressor

[a] Dissociation rates, mean from at least three iterations, were obtained by curve fitting the observed kinetics from individual iFRAP experiments with an exponential decay algorithm (Rabut 2004).
[b] Structural residence time was calculated via $1/k_{(off)}$ and is the time at which 50% of fluorescence is lost.
[c] Rap1 contributes to telomere silencing.

The integral membrane protein Pom34 was second fastest among the NPC factors exhibiting a structural residence time of 40s. This result was surprising since Pom34 is an integral membrane protein that constitutes a portion of the NPC scaffold. However, this apparent contradictory result has been seen before in a similar study where human hGp210, an integral membrane protein involved in NPC site selection (Rabut *et al.* 2004),

was also observed to have relatively fast structural dissociation kinetics. Interestingly, the last three NPC components tested, who have all been shown to contribute to gene regulation, exhibited the most stable structural association to the pore complex.

Acetyl Exchange Factors Quickly Dissociate From Their Canonical Nucleosomal Target, Histone 2B

The next nuclear factors I observed were chromatin factors. Since genes relocate to the nuclear periphery, it stood to reason that perhaps factors involved in converting inactive heterochromatin to active euchromatin might also associate with perinuclear structures. Htb2, encodes Histone 2B in yeast, contributes to the formation of the histone complex that constitutes the foundation of nucleosomes. Though Htb2 is largely nucleoplasmic and has been shown not to interact directly with the nuclear periphery (Sarma *et al.* 2007). I expected Htb2 to exhibit a slow dissociation rate as it is mostly compacted within dense heterochromatin. Conversely, the SAGA component, Sgf73, I hypothesized to interact with more stable structures at the periphery in order to perhaps facilitate remodeling of target promoters for activation. What I observed was that the residence time of Htb2 was indeed relatively high, indicative of a low rate of exchange (Table 2). Interestingly, the observed kinetics suggest that histone incorporation into nucleosomes is as structurally stable as nucleoporins are to the NPC (Figure 7B). Conversely, for the acetylation factors, Hda1 and Sgf73 both exhibited a much lower residence time (Figure 7C and Table 2).

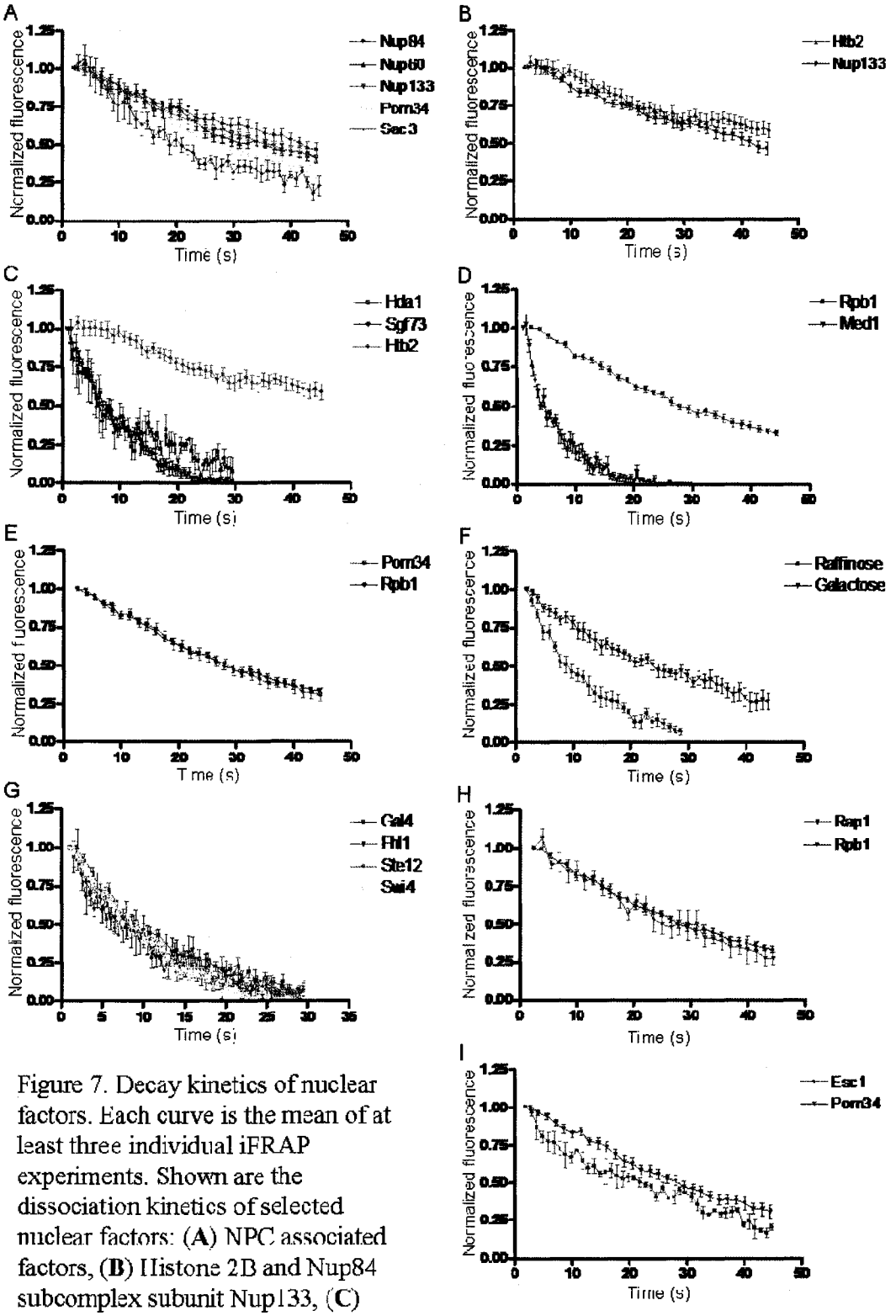

Figure 7. Decay kinetics of nuclear factors. Each curve is the mean of at least three individual iFRAP experiments. Shown are the dissociation kinetics of selected nuclear factors: (**A**) NPC associated factors, (**B**) Histone 2B and Nup84 subcomplex subunit Nup133, (**C**) Histone 2B and associated acetylation factors, (**D**) largest subunit of Pol II Rpb1 and Mediator component Med1, (**E**) integral membrane protein Pom34 and Rpb1, (**F**) Gal4 kinetics in uninduced (raffinose) and induced (galactose) conditions, (**G**) various transcriptional activators, (**H**) transcriptional regulator Rap1 and Rpb1 and (**I**) silencing factor Esc1 and the integral membrane protein Pom34.

Components of the Polymerase II Holoenzyme Show Distinct Kinetic Differences

We were next interested in looking at components of the transcriptional machinery. If reverse recruitment provides a robust model for gene regulation, we expect that the transcriptional machinery, or at least the core components of Mediator and Pol II, would be predominately immobile. What we observed, however, was that Med1 of the Mediator, and Rpb1 of the Pol II complexes showed a 9 fold difference in structural residence time (Table 2; Figure 7D) despite the fact that they both co-fractionate with the nuclear periphery (see below). The Pol II large subunit Rpb1 showed a very similar kinetic profile to the integral membrane protein Pom34 (Figure 7E). Importantly, this observed structural retention of Rpb1 is consistent with its functional association with the nuclear periphery (see below) and our expectations with the reverse recruitment model. Conversely, Med1, shown to interact with the Mediator core subunits Med4 and Med8 (Balciunas *et al.* 2003), exhibited a residence time of only 5.5s. It is therefore likely that Med1 is a transient factor in the Mediator complex. In order to clarify this discrepancy a more comprehensive study of the Mediator subunits would be needed.

Transcriptional Regulators Vary Greatly in Their Dissociation Kinetics

The last part of the puzzle that we wanted to address with iFRAP deals with transcriptional regulators. It is unclear as to the fate of the activator or repressor while fulfilling its regulatory role. In the context of the recruitment model, kinetic expectations would be that a regulator would maintain a level of free diffusion in order to efficiently come in contact with its target genes. However, in the reverse recruitment model we predict that activators are capable of slower kinetics while associated with the immobile

transcriptional machinery (see above). Conversely, repressors function to inhibit this productive association between transcriptional machinery and target genes, therefore they are predicted to be generally mobile. What I found is that for cells grown in galactose (induced), the transcriptional activator Gal4 does in fact shift to a more stably bound form (Figure 7F), indicative of structural integration (see below). When cells are grown in raffinose (in uninducing media), Gal4 matched the kinetic profiles of Ste12, Swi4 and Fhl1 (Figure 7G), suggesting that the latter three factors may likewise be inactive. However, in order to support this possible correlation between these distinct regulatory pathways, more experimentation would have to be done. I also found that the constitutively active Rap1 and glycolytic activator Gcr1 exhibit a structural residence time nearly identical to that of Rpb1 (Figure 7H; Table 2).

The promoter specific, DNA-binding repressor Mig1 was found to have a very low residence time of 5.88s. Mig1 binds to the co-repressor Ssn6 (Treitel and Carlson 1995) which in part mediates repression via histone deacetylation (Wu *et al.* 2001). Interestingly, Ssn6 showed a 10s residence time, twice that of Mig1 and similar to the Hda1 residence time of 9s (Table 2). Interestingly, for cells grown in pyruvate (relieving glucose repression) Ssn6 appeared to show a slightly less structural residence time of ~7s. Since glucose repressed genes are only a subset of Ssn6 targets (Huang *et al.* 1998; Proft *et al.* 2001; Treitel and Carlson 1995), this minor shift in kinetics is consistent with Ssn6 remaining active, though perhaps to a lesser degree. Lastly, I examined the telomere silencing factor Esc1. Telomere silencing occurs at the nuclear periphery and requires Esc1 to assist in anchoring (Taddei *et al.* 2004). The Esc1 dissociation profile was

consistent with this reported function as it exhibited a structural residence time comparable to that of the integral membrane protein Pom34 (Table 2; Figure 7I).

CHAPTER IV

CHROMOSOME DYNAMICS OF *SUC2*

Reverse Recruitment of SUC2 to the Nuclear Periphery

Recent work has clearly demonstrated that transcriptionally active target genes in *S. cerevisiae* (e.g., those regulated by Rap1/Gcr1, Gal4, and Ino2) physically associate with perinuclear factors (Brickner and Walter 2004; Casolari *et al.* 2004; Menon *et al.* 2005). Given the data presented above, we suspected that *SUC2*, the canonical glucose-repressed locus on chromosome IX, might also be associated with the nuclear periphery when active. We tested this by inserting an array of lac operators upstream of *SUC2* in cells that expressed a LacI repressor fused to green fluorescent protein (LacI-GFP); this allowed monitoring of the *in vivo* subnuclear position of the tagged locus within a confocal optical slice (Figure 5). Co-expression of a YFP-tagged nucleoporin (Nsp1-YFP) allowed simultaneous visualization of the nuclear periphery.

In glucose-grown cells (under repressing conditions), the location of *SUC2* in the nucleus appeared to be random; it was present in the perinuclear compartment (taken as the outer third of the nuclear area; see Taddei et al. 2006) in 45% of cells (Table 3; n = 153). In the absence of glucose (under derepressing conditions), when expression is ~100-fold higher, *SUC2* localization to the perinuclear compartment increased to 74% (Table 3; n = 143; $P < 0.0001$). Time lapse fluorescence microscopy revealed a striking carbon source-dependent difference in the intranuclear motility of *SUC2*. The position of *SUC2* was dynamic in glucose-grown cells (Figure 8A). However, in the absence of

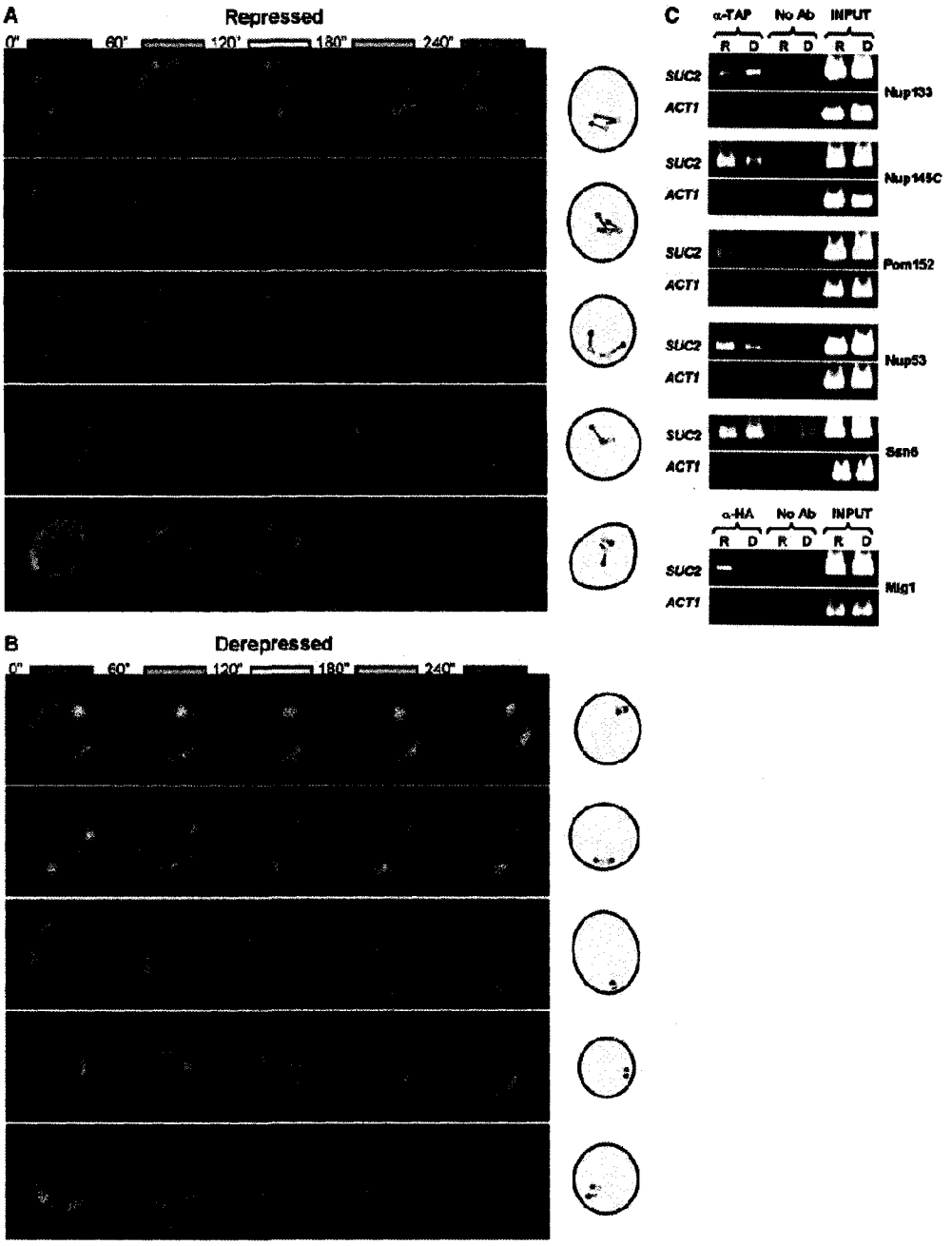

Figure 8. *SUC2* exhibits carbon-source-dependent motility and associates with NPCs. Time-lapse analysis (4 min total) of the location of GFP-tagged *SUC2* in either (A) repressed or (B) derepressed cells is shown; the result for each of five different nuclei in either repressing or derepressing conditions is presented horizontally in temporal order from left to right. The cartoon on the right depicts the location of the gene within the nucleus at the time indicated, in seconds: 0 (blue), 60 (green), 120 (yellow), 180 (orange), and 240 (red). A YFP fusion to the essential NPC component Nsp1 marks the nuclear periphery. (C) ChIP analysis of association between *SUC2* and factors that represent different strata of the nuclear periphery. TAP-tagged Nup53 (NPC subunit), Nup133 (NPC subunit), Nup145 (NPC subunit), Pom152 (NPC-specific integral nuclear

membrane protein), or Ssn6 (perinuclear Mig1 corepressor; see Figure 2E), or HA-tagged Mig1, were immunoprecipitated from cells grown on either the presence (R, repressed) or absence (D, derepressed) of glucose. The *SUC2* promoter and ACT1 (negative control) promoter were amplified from both immunoprecipitated material and whole-cell extracts (INPUT, positive control). No Ab, no antibody (negative control).

glucose, movement of *SUC2* was restricted to the perinuclear compartment, including occasional sliding along the nuclear periphery (Figure 8B). Although the underlying explanation for this lateral perinuclear sliding remains to be determined, similar behavior has also recently been reported for other transcriptionally active genes (Cabal *et al.* 2006; Taddei *et al.* 2006).

Chromatin immunoprecipitation (ChIP) data (Figure 8C), which were verified across a three-fold range of PCR template, show that the *SUC2* promoter associates with at least four different components of the NPC (Nup53, Nup133, Nup145C, and Pom152; Figure 8C) in both the presence and the absence of glucose; removal of some of these same factors impairs both repression and derepression of *SUC2* (see below). *SUC2* is also constitutively associated with the corepressor Ssn6 (Figure 8C). In contrast, *SUC2* associates with Mig1 only in the presence of glucose; this was expected because Mig1 is exported to the cytoplasm in the absence of glucose (De Vit *et al.* 1997). Interestingly, Act1, used as our negative ChIP control, is a highly expressed gene but fails to interact with the NPC (Figure 8C). Providing at least one instance where interaction with the NPC appears to be dispensable for gene regulation.

Mig1 repression occurs in the perinuclear compartment

Many glucose-regulated genes are transcriptionally repressed by the DNA-bound factor Mig1 (Lutfiyya *et al.* 1998). In glucose-grown *Δmig1* cells, *SUC2* expression was ~20-fold higher than in wild type (Vallier and Carlson 1994). I found that this increase in

expression corresponds with a significant increase in the peripheral localization of the ORF; the gene is localized to the nuclear periphery in 60% of *Δmig1* cells (n = 146) vs. 45% of glucose-grown wild-type cells (n = 152, $P < 0.01$; Table 3). In agreement with previous reports (De Vit *et al.* 1997), confocal microscopy-based analysis showed Mig1-GFP to be nuclear in the presence of glucose and cytoplasmic in the absence of glucose (Figure 9A). Quantitative fluorescent protein detection (QFPD) analysis, a technique used to measure subcellular protein distribution after biochemical fractionation (Sarma *et al.* 2007), enables the assaying of theoretically any one of the ~4000 genes tagged with GFP contained with the yeast GFP cloning library. This technique further allowed us to quantitate the presence of a target protein within each of the cytosolic, nucleic and nuclear envelope compartments. QFPD analysis revealed found that Mig1 is nuclear in glucose grown cells (Figure 9B), i.e., when it binds upstream of *SUC2* (Figure 8C) and represses transcription (Carlson 1999; Turkel *et al.* 2003). Interestingly, QFPD analysis further showed that the perinuclear compartment contains a substantial fraction of Mig1 (Figure 9B). This suggests that repression by Mig1 is a dynamic process that requires association with both the promoter DNA and the nuclear periphery (see Discussion). In the absence of glucose (derepressing conditions), Mig1 exited the perinuclear compartment (Figure 9B) a result that agrees with its observed relocation to the cytoplasm (Figure 9A; see above).

Deletion of *HXK2*, which encodes the predominant form of hexokinase in S. cerevisiae, has long been known to cause defects in glucose repression (Entian 1980). In *Δhxk2* cells grown on glucose, invertase activity increased dramatically (Table 3; Neigeborn and Carlson 1984) this increase remains unaltered in *Δhxk2 Δmig1* cells

Table 3: Increased *SUC2* expression correlates with increased localization of the gene to the nuclear periphery

	SUC2 expression[a]		% cells with peripheral SUC2 ORF[b]	
Genotype	R (glucose[c])	D (no glucose[c])	R (glucose[c])	D (no glucose[c])
WT	2.6 ± 0.2	267.2 ± 31.3	45	74
Δmig1	52.8 ± 8.8	148.4 ± 1.8	60*	69
Δhxk2	65.4 ± 8.2	164.1 ± 36.6	60**	72

[a] *SUC2* expression was measured with invertase assays as described in Neigeborn and Carlson (1984). Error denotes the standard deviation of four determinations.

[b] Percentage of cells where the *SUC2* ORF is localized to the outer third of the nucleus. P-values, calculated on the basis of a two-tailed Student's t-test, represent a significant difference in the localization of the ORF in glucose-grown *WT* cells relative to glucose-grown *Δmig1* or *Δhxk2* cells. *Significant ($P < 0.01$); **highly significant ($P < 0.0005$). At least 115 cells were measured for each condition.

[c] See materials and methods for growth conditions.

(Sarma 2007). Thus, despite its presence in the nucleus of glucose-grown *Δhxk2* cells (Figure 9A), Mig1 has lost its function as a repressor. Strikingly, QFPD analysis of Mig1-GFP demonstrated that nuclear Mig1 is depleted from the perinuclear fraction of glucose-grown *Δhxk2* cells (Figure 9B), indicating that the repressor function of Mig1 requires its presence in the perinuclear compartment. Consistent with this result, *SUC2* is retained at the nuclear periphery in 60% ($n = 150$) of glucose-grown *Δhxk2* cells (Table 3), a significant increase over that in glucose-grown wild type cells ($P < 0.0005$). In the absence of glucose, *SUC2* is retained at the periphery in 72% of *Δhxk2* cells ($n = 158$); thus in derepressed conditions, both the perinuclear localization of the gene and expression levels (Neigeborn and Carlson 1984) are comparable in the presence and absence of Hxk2.

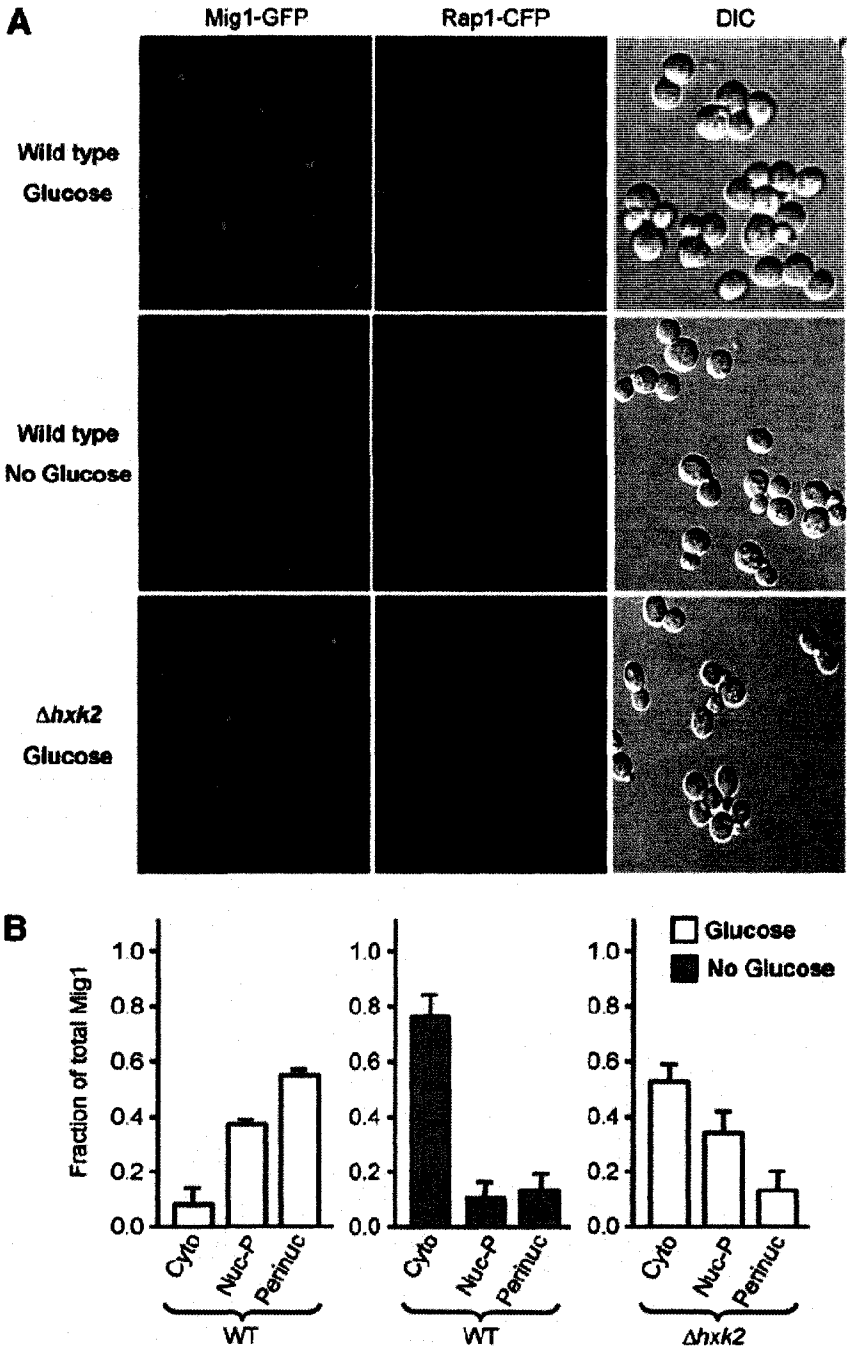

Figure 9. Perinuclear localization is required for repression by Mig1. (A) Confocal laser scanning microscopy of Mig1-GFP in wild-type or *Δhxk2* cells grown in either the presence or the absence of glucose, as indicated; coexpressed Rap1-CFP is shown as a nuclear marker. GFP and CFP signals were captured by using a Zeiss LSM 510 META confocal laser scanning microscope with a 63x Plan-Apochromat 1.4 NA oil DIC objective lens. (B) Graphs show the fraction of total Mig1-GFP fluorescence present in cytoplasmic (Cyto), nucleoplasmic (Nuc-P, total nuclear fluorescence minus perinuclear fluorescence), and perinuclear (Perinuc) fractions, as determined by QFPD analysis. Open bars, glucose; shaded bars, no glucose. Error bars represent the standard error of the mean.

CHAPTER V

CHROMOSOME DYNAMICS OF *GAL1*

Peripheral Anchoring of *GAL1* is Induction Dependent

Using the GFP gene tagging technique, *GAL* genes have been shown to move to the nuclear periphery upon galactose induction (Figure 10; Cabal *et al.* 2006; Dieppois *et al.* 2006). Several lines of evidence suggest that the Gal4 activator is responsible for this directed gene relocation. An interaction between Nups and the *GAL1, 10* promoter (Nup-PI) requires Gal4 and its binding site in DNA (Schmid *et al.* 2006). Chromatin immunoprecipitation confirms that the *GAL1, 10* promoter, but not the adjacent *GAL1* or *GAL10* ORFs, contact several nucleoporins (including Nup84; our unpublished data). Measurement of the nuclear position of GFP-tagged *GAL* genes (the *GAL1, GAL10* and *GAL7* cluster on chromosome 2), as well as time lapse analyses (not shown), indicated that movement of *GAL* genes to the nuclear periphery is eliminated in the absence of Gal4, whereas perinuclear anchoring of *GAL* genes is constitutive in *gal80*Δ cells (Figure 10B). The latter result is consistent with the well-established role of Gal80 repressor, which binds to and inhibits the primary Gal4 activation domain, thereby blocking *GAL* gene transcription in wild type cells grown in the absence of galactose (Pilauri *et al.* 2005).

Movement of *GAL1* to the Periphery Precedes Expression

As stated previously, induced or derepressed genes move to the nuclear periphery. However, an important aspect of this movement remained unaddressed: whether or not gene relocation precedes or follows expression. Traditionally, it was only possible to observe either the gene localization or expression independently. To answer this question

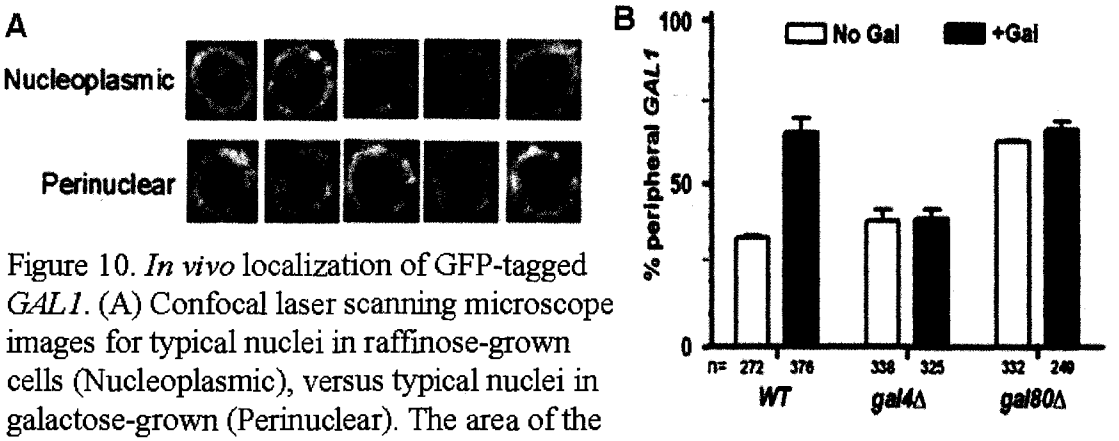

Figure 10. *In vivo* localization of GFP-tagged *GAL1*. (A) Confocal laser scanning microscope images for typical nuclei in raffinose-grown cells (Nucleoplasmic), versus typical nuclei in galactose-grown (Perinuclear). The area of the nucleus captured in each confocal slice is divided into thirds; the GFP-tagged GAL1 gene (green spot) is counted as perinuclear if it appears in the outermost third of the nuclear area. Nsp1-YFP (yellow ring) marks the nuclear periphery. (B) *In vivo* localization of GFP-tagged *GAL1* in wild type or mutant cells grown on uninducing media (raffinose, open bars) or inducing media (galactose, +Gal, filled bars). Bars represent the proportion of *GAL1* loci found in the peripheral third of the nucleus; the number of cells analyzed for each condition is indicated below each bar.

however, we needed a way of monitoring both simultaneously. To do this, I augmented the GFP gene tagging technique, by replacing the *GAL1* ORF with a fluorescent cell membrane protein (GFP-Ras2) that would serve as a galactose regulated expression reporter (Figure 11). We chose Ras2 as our reporter because it is located within a separate cell compartment than the gene tracking probe. Additionally, these cells contained Nup49 and Nup60 both fused with tDimer2, which is a homodimeric variant of DsRed, to mark the nuclear periphery.

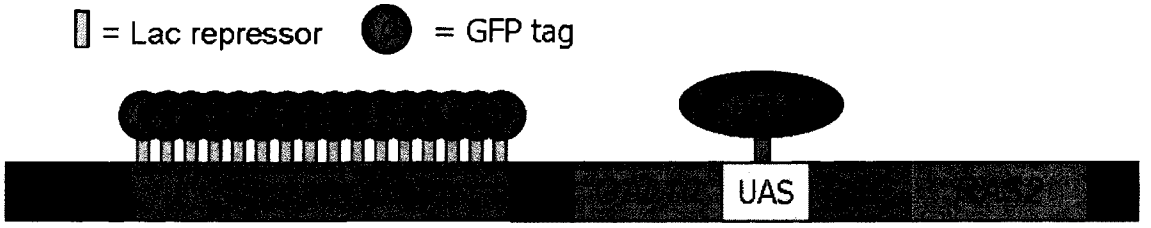

Figure 11. Galactose induction drives the cellular membrane fluorescent reporter GFP-*RAS2*. Gene tagging was accomplished as previously described (Figure 2). Replacement of the *GAL1* coding region (*GAL1:GFP-RAS2)* was accomplished by recombination cloning. Expression of *GFP-RAS2* is regulated by the native Gal4/Gal80 mechanism.

This "single cell" assay allowed us to monitor simultaneously both *GAL* gene location and GFP-Ras2 expression levels in individual cells. Preliminary observations with this technique were consistent with previous findings: cells grown in the absence of galactose (uninduced) showed random *GAL* gene mobility, whereas in the presence of galactose (induced) the *GAL* genes were both peripheral and transcriptionally active, indicated by GFP fluorescence at the cell surface (Figure 12).

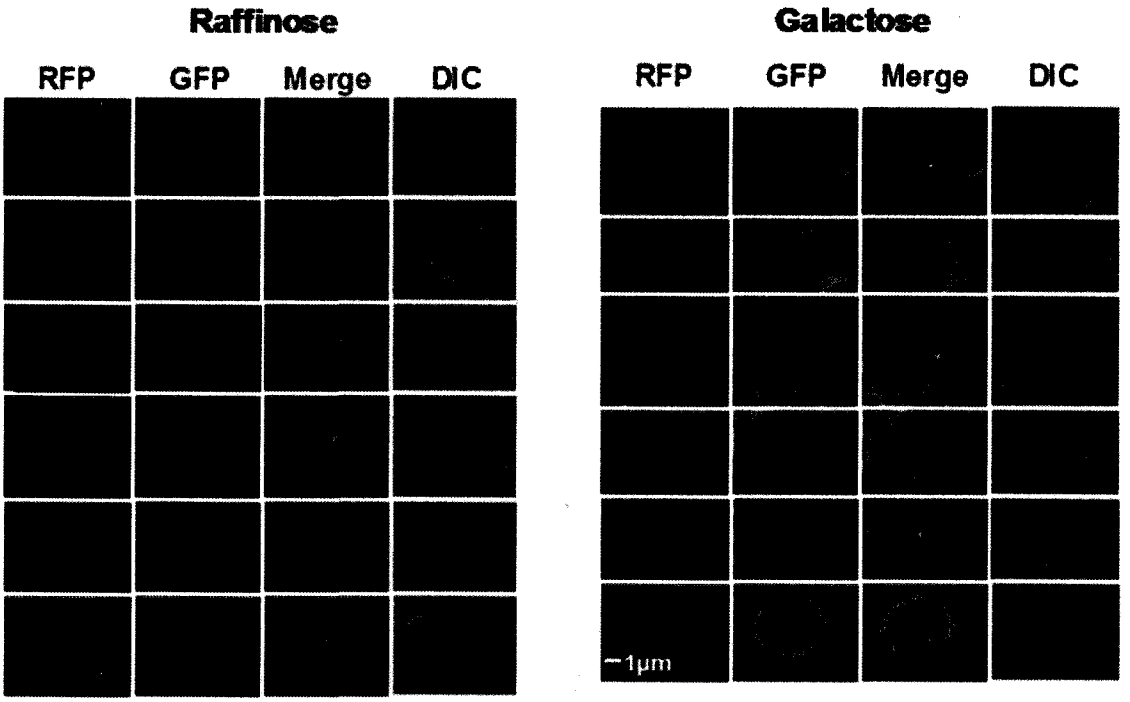

Figure 12. GFP-tagged *GAL1* promoter (green spot) drives galactose-induced expression of the GFP-*RAS2* product, which is tightly localized to the plasma membrane (outer green ring). The nuclear periphery of strain KB12 is marked with Nup49-tDimer2 and Nup60-tDimer2 (red ring); GFP tagging of the *GAL1:GFP-RAS2* locus was done as described (Figure 8). Left panel, uninducing media (SC+Raffinose). Right panel, inducing media (SC+Galactose). CLSM images for six KB12 cells in each panel, left panel: tDimer2, GFP, Merge (tDimer2+GFP), DIC.

This single cell assay could be used to examine the timing involved in expression and peripheral localization of the *GAL* genes, which was exactly our goal in order to address our question of when does active gene expression correlate with peripheral

localization. I grew cells in 3% raffinose to an OD_{600} of 0.8, at time zero added galactose to a final concentration of 3% and at intervals after the addition of galactose I harvested cells and imaged them for the location of the *GAL* genes and *GFP-RAS2* expression and found that *GAL* gene localization to the periphery occurs within 15 minutes of exposure to galactose, increasing to 65% ± 1% (n = 98; Figure 13A) at 60 minutes, which is in agreement with previous work (Brickner *et al.* 2007; Drubin *et al.* 2006). It has been shown that *GAL1* mRNA transcripts increase slightly between 30 and 60 minutes following galactose induction, then accumulate sharply (Brickner *et al.* 2007). In this assay we saw fluorescence of GFP-Ras2 quickly increases from 30 minutes to steady state levels at 120 minutes (blue dashed line in Figure 13A), again in agreement with previous work.

The reverse recruitment model postulates that genes move to the nuclear periphery to become transcriptionally active. This predicts that translocation to the nuclear periphery is required prior to expression. If this is true, using the single cell assay, we expect that cells exhibiting perinuclear *GAL* genes will become active sooner than those found to be nucleoplasmic. What we observed is that between 30 and 60 minutes the number of cells with an active peripheral gene increased sharply in comparison to the cells with genes located in the nucleoplasm (Figure 13B). Interestingly, at 90 minutes there was a peak in the accumulation of nucleoplasmic expressors, perhaps indicating an attenuation of expression through feedback in the pathway. The data in Figure 13B suggests that those cells in which the *GAL* genes are located near the nuclear periphery exhibit an overrepresentation in active *GFP-RAS2* expression compared to nucleoplasmic *GAL* genes. To investigate this possibility in more detail, we repeated the experiment and

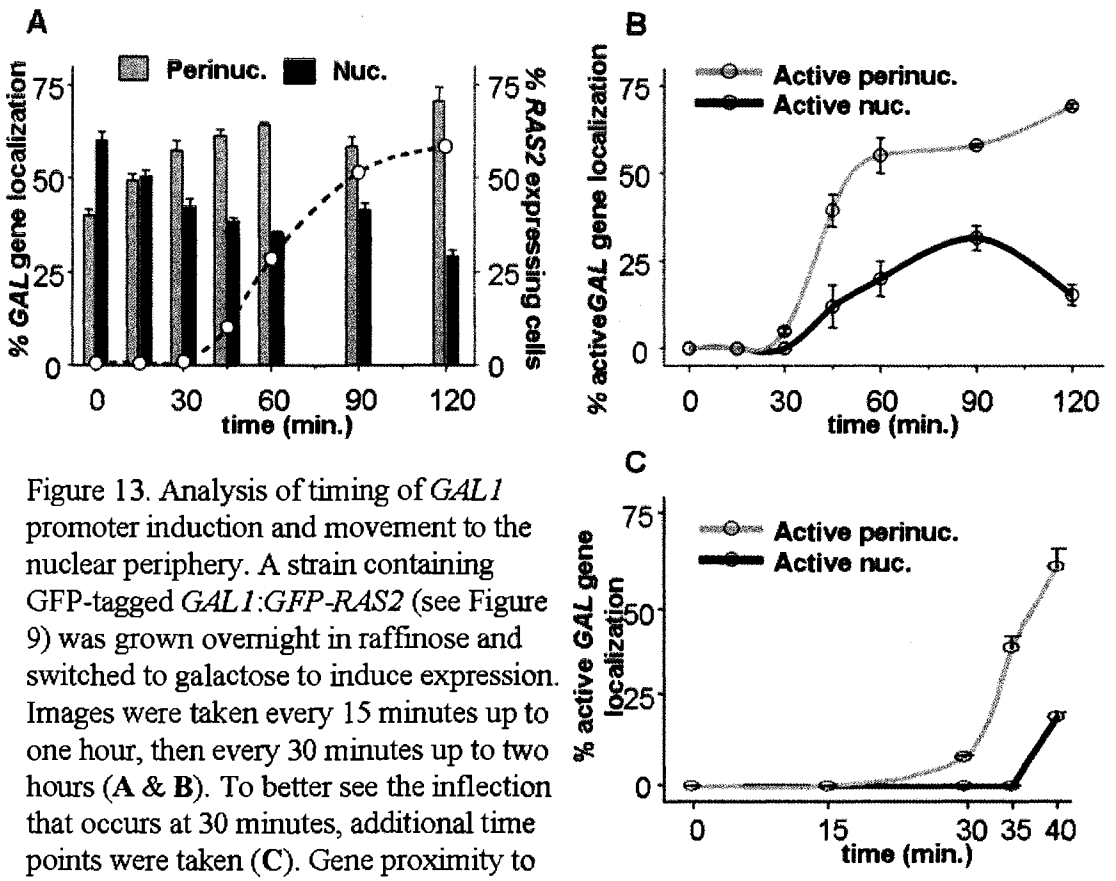

Figure 13. Analysis of timing of *GAL1* promoter induction and movement to the nuclear periphery. A strain containing GFP-tagged *GAL1:GFP-RAS2* (see Figure 9) was grown overnight in raffinose and switched to galactose to induce expression. Images were taken every 15 minutes up to one hour, then every 30 minutes up to two hours (**A** & **B**). To better see the inflection that occurs at 30 minutes, additional time points were taken (**C**). Gene proximity to the nuclear periphery was determined as previously described (see Figure 7A) and classified as being Perinuclear (**A**; gray bar) or Nucleoplasmic (**A**; black bar). The blue dashed line represents the percentage of cells exhibiting GFP-Ras2 fluorescence. The appearance of GFP-Ras2-expressing perinuclear genes (gray line) or nucleoplasmic genes (black line) was monitored during the first two hours following the appearance of galactose (**B**). This analysis was repeated with additional timepoints during the first 40 minutes (**C**).

looked at 5 minute time intervals after 30 minutes. Strikingly, we see that at 30 minutes, all expressing cells were observed to contain perinuclear *GAL* genes (Figure 13C) suggestive of pre-expression anchoring. Further, active nucleoplasmic *GAL* genes were not observed until 10 minutes later.

Anchoring of *GAL1* is Independent of Transcription

The above experiment suggested that perinuclear gene localization occurs prior to expression of the gene product. While the result is clear and in agreement with a reverse

recruitment mechanism, the single cell analysis does not directly address the activity of the transcriptional machinery itself or its subnuclear localization. We attempted to answer this question by observing the motility of GAL genes upon inducing conditions during a transcriptional block. For this experiment we utilized the *rpb1-1* temperature sensitive mutant (Nonet *et al.* 1987). In this mutant, transcription occurs at the permissive temperature (30°C) but is completely blocked at the non-permissive temperature (37°C). If *GAL* genes relocate to the nuclear periphery following galactose induction in *rpb1-1* cells held at the non-permissive temperature, then transcriptional activity is most likely not a prerequisite for perinuclear anchoring. This is exactly what we observed (Figure 14A-D); perinuclear anchoring occurs identically in the presence and absence of *GAL* gene transcription. Cells grown in raffinose at the permissive temperature were observed to have highly mobile *GAL1* gene and no detectible transcript (determined through Northern analysis; Figure 14A). When switched to the non-permissive temperature for 1 hour, the *GAL1* continues to be highly mobile and uninduced (Figure 14B). In order to maintain this strict shutoff of *rpb1-1* while performing microscopy, all cells were kept at 37°C using a stage warmer. Next, while kept at the non-permissive temperature and exposed to galactose, cells exhibited perinuclear *GAL1* even in the absence of transcription (Figure 14C). Strikingly, we can observe this intermediate state of activation for 4 hours (Figure 14D). Finally, a subsequent shift to the permissive temperature permited *GAL1* transcription to initiate normally while the gene remains anchored (Figure 14E). These data are consistent with the observation that *GAL* gene anchoring at the periphery precedes the appearance of the corresponding transcript (Brickner *et al.* 2007). Similar evidence, including gene anchoring upon induction in *rpb1-1* cells held at

the non-permissive temperature, has also been reported for *INO1* (Brickner *et al.* 2007), a gene that is transcriptionally regulated in response to inositol levels.

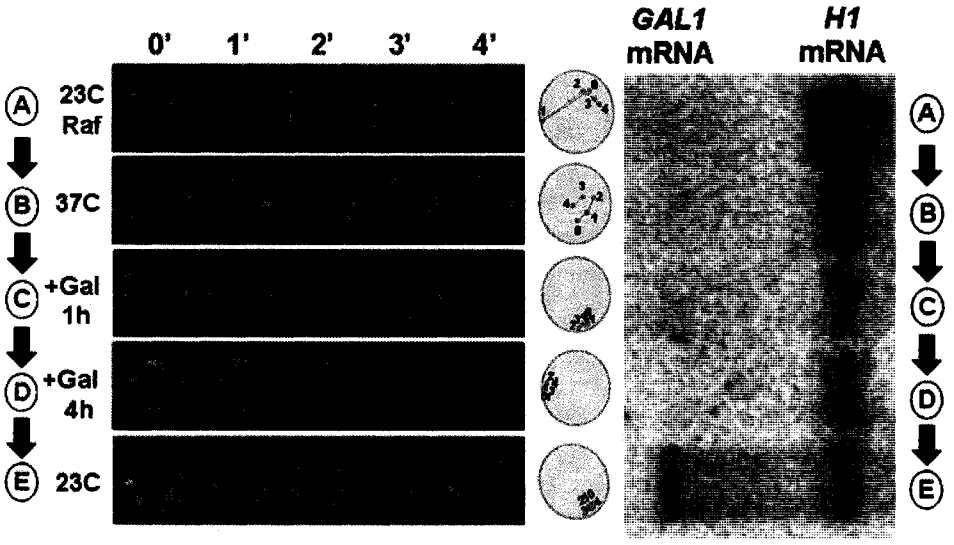

Figure 14. Perinuclear anchoring of *GAL1* in the absence of transcription. The left panel shows five time lapse series of representative nuclei from temp.-sensitive *rpb1-1* cells; the cartoon to the right of each series of images indicates the position of the *GAL1* gene spot (see text) within each nucleus at each of the four time points (0, 1, 2, 3 and 4 minutes). The right panel shows the corresponding Northern blot analysis for each condition; the stable mRNA encoding histone H1 was included as a control. Cells were initially grown at the permissive temp. in synthetic complete media supplemented with the uninducing sugar raffinose (**A**; 23C/Raf). As in wild type cells (Cabal *et al.* 2006), the uninduced *GAL1* gene is highly mobile in the *rpb1-1* strain. A one hour shift to the non-permissive temp. (**B**; 37C) results in complete shutoff of transcription (Nonet *et al.* 1987). The inducing sugar galactose was added while maintaining the cells at the non-permissive temp. (+Gal); anchoring of *GAL1* at the nuclear periphery was observed after one hour (**C**) and persisted for more than four hours (**D**) despite maintenance of the transcriptional block. Finally, after a shift back to the permissive temp. (**E**; 23C) the gene remains anchored at the nuclear periphery while transcription of *GAL1* commences.

Components of the Pre-initiation Complex (PIC) Co-fractionate with NPC Components

Taken together these data suggest that perinuclear anchoring may be a common feature of gene induction. If this is true, there should be a functional and potentially physical association of the general transcriptional machinery, particularly RNA

polymerase II (Pol II), with the NPC; we therefore used a nuclear envelope purification protocol (Kipper *et al.* 2002) to test directly for co-fractionation of components of the Pol II pre-initiation complex (PIC; comprised of Mediator, TFIID and Pol II) with NPCs. This technique allowed us to examine the enrichment of the tested proteins specifically within the nuclear envelope. For our positive and negative controls, we chose the nuclear membrane NPC component Pom152 and nucleolar factor Nop1, respectively. All observed protein enrichment to the nuclear envelope was quantified by densitometry and then normalized as a percentage of Pom152.

Using this technique, each of the seven PIC components we have thus far attempted to detect in nuclear envelope fractions, including Ssn8/Srb11, co-fractionated efficiently with the nuclear membrane-embedded NPC component Pom152 (Menon *et al.* 2005; Sarma *et al.* 2007), and was at >50-fold higher levels in perinuclear fractions than the negative control (Nop1; Figure 15A). This apparent tethering of the transcriptional machinery to NPCs does not respond to changes in carbon source, for example growth on glucose vs. galactose (Buford and Santangelo; unpublished data). However, as mentioned above regarding perinuclear tethering of the induced genes themselves, it is possible to argue that concentration of the transcriptional machinery at the nuclear periphery is not a prerequisite for, but is instead a consequence of, gene activation. This seems unlikely because our fractionation protocol includes a DNase step, which should release transcription factors that are tethered to the nuclear periphery only as a consequence of their interaction with actively transcribing genes (Menon *et al.* 2005; Sarma *et al.* 2007). Nevertheless, we tested this possibility further by repeating the nuclear fractionation experiment with *rpb1-1* cells held at the non-permissive temperature for four hours,

reasoning that a prolonged transcriptional block would result in a detectable reduction in steady-state levels of perinuclear PIC components if their presence in nuclear envelope fractions was merely a consequence of active gene transcription. Representative results are shown in Figure 15B; transcriptional shutoff has little or no effect on the co-fractionation of PIC components with perinuclear factors.

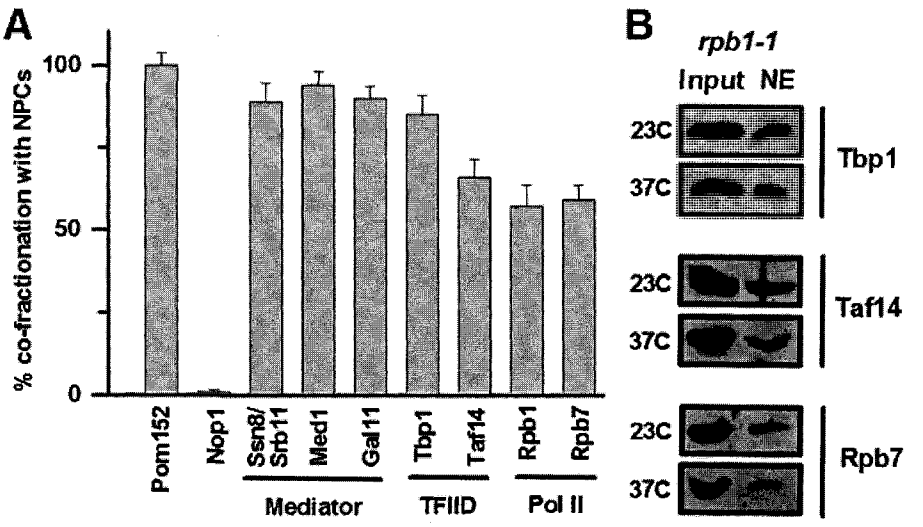

Figure 15. Components of the Pol II pre-initiation complex (PIC) co-fractionate with NPCs. PIC components were detected in nuclear envelope fractions via epitope tags or native antibodies. (**A**) Amount of protein in the nuclear envelope fraction, relative to the total nuclear fraction, was determined densitometrically and normalized to the value for the integral nuclear membrane protein Pom152, which was set to 100%. The nucleolar protein Nop1 is shown as a negative control. (**B**) Western analysis of PIC components Tbp1, Taf14 and Rpb7 in total nuclear fractions (Input) and nuclear envelope fractions (NE); *rpb1-1* cells were harvested either immediately before (23C) or four hours after a shift to the non-permissive temp. (37C).

CHAPTER VI

MODULAR GAL4 DOMAIN ANALYSIS

The previous chapter suggested the intriguing new possibility that association of Gal4 with the nuclear periphery might play an important role in the induction of target genes by this classical yeast activator. We therefore also tested Gal4 co-fractionation with perinuclear factors. We found that wild type Gal4 does indeed associate with NPCs in induced (galactose-grown) but not in uninduced (raffinose-grown) cells (Figure 16A). Similar to the tethering of *GAL* target genes at the nuclear periphery, upon removal of Gal80, this co-fractionation of Gal4 with NPCs becomes constitutive (Figure 16A).

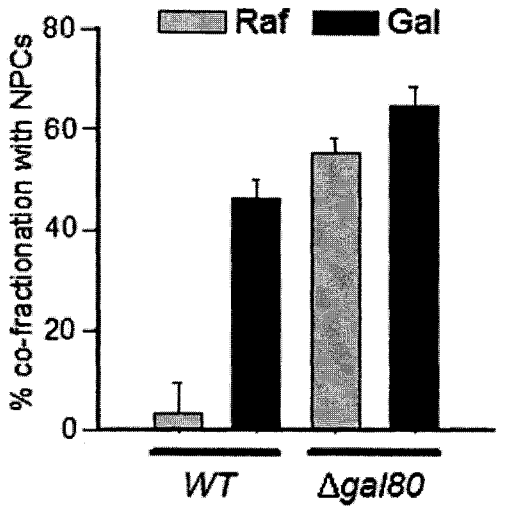

Figure 16. Gal4 co-fractionation with perinuclear factors. After detection of wild type and mutated Gal4 in both nuclear envelope fractions and total nuclear fractions via epitope tag, ratios were determined by densitometry and normalized to the corresponding values for the integral nuclear membrane protein Pom152, which was set to 100%. Co-fractionation with NPCs was determined for wild type Gal4 in *GAL80* (*WT*) and *Δgal80* cells grown in uninducing (SC+Raf) and inducing (SC+Gal) media.

We next reasoned that stable association between Gal4 and a very large membrane-embedded structure like the NPC (>60 MDa in *S. cerevisiae*; Kiseleva *et al.* 2004) might result in a detectable change in the mobility of Gal4. As mentioned above, FRAP analysis

determines the strength of *in vivo* binding interactions by measuring protein mobility (i.e. the molecular dynamics of diffusion; (Sprague and McNally 2005; van Drogen and Peter 2004). We hypothesize that the incorporation of a nuclear protein such as Gal4 into a multi-subunit complex that is freely diffusing would have only a small effect on mobility. Conversely, larger effects would indicate possible interactions with an immobile component of the nucleus (Misteli 2001), such as the NPC. FRAP analysis was performed on cells grown in either uninducing (3% raffinose) or inducing conditions (3% galactose). Representative images of the fluorescent recovery are shown in Figure 17A & B. FRAP analysis of Gal4-GFP, which is fully functional (see below), exhibited a galactose-dependent reduction in diffusion rate (Figure 17C). Quantitation of the FRAP data collected with the Zeiss CLSM indicated that structural association of Gal4-GFP in the presence of galactose is comparable to the constitutive, stable incorporation of histone H2B into chromatin (Figure 17E), a major immobile component in the nucleus (see above; Misteli 2001). Diffusion of the GFP protein by itself is rapid (i.e. post bleaching, GFP was fully redistributed in under 250ms) and unaffected by carbon source. Further, in cells lacking Gal80, structural association of Gal4, similar to its co-fractionation with NPCs, becomes constitutive (Figure 17D, E).

Perinuclear anchoring of the Gal4 protein, and the failure of *GAL* genes to do so in Δ*gal4* cells, suggested that Gal4 might mediate movement of target genes to the nuclear periphery upon induction. This is the predicted function of a "perinuclear shuttling factor", a class of transcriptional regulators whose existence we postulated based upon the mechanism of Snf1/Mig1 glucose repression (Sarma *et al.* 2007). However, an alternative explanation was that an as yet unidentified factor is primarily responsible for

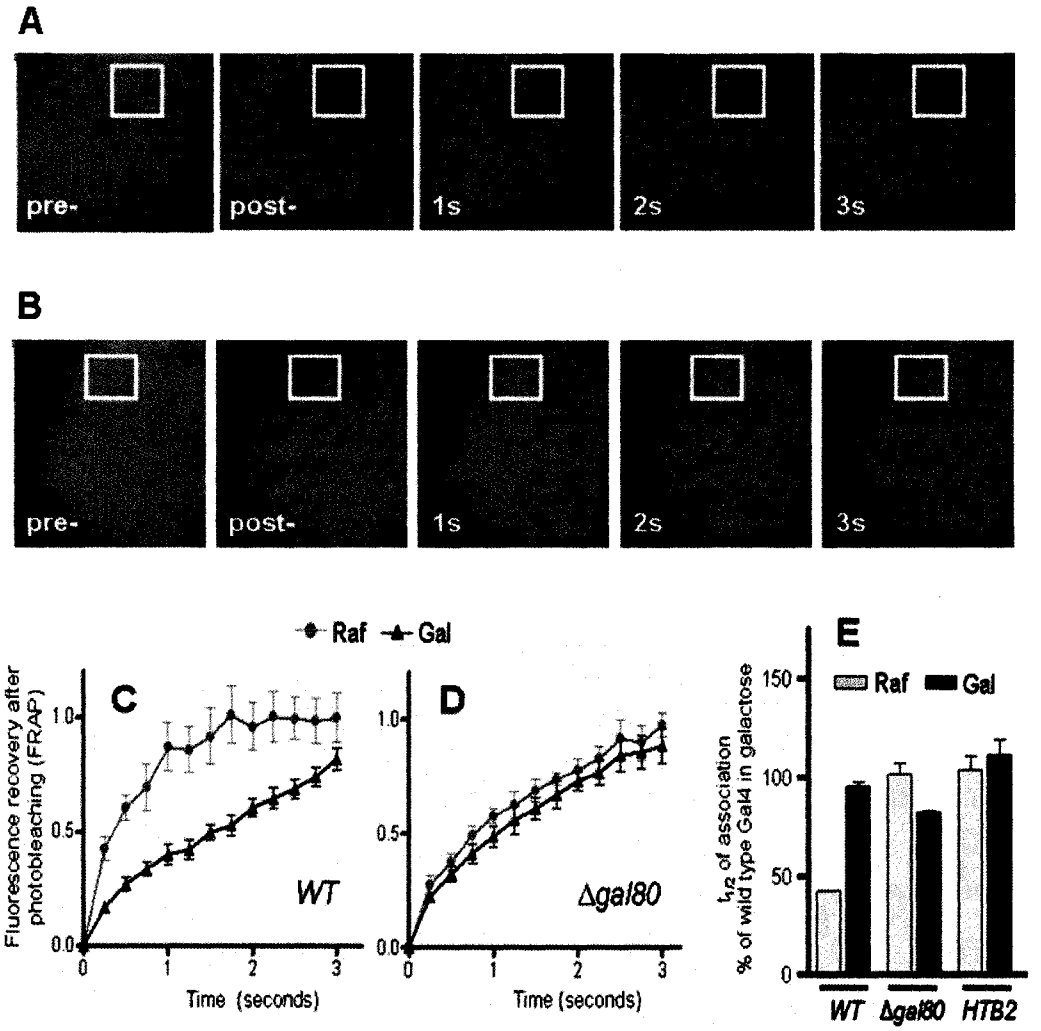

Figure 17. *In vivo* association of Gal4 with nuclear structures. A Zeiss confocal laser-scanning microscope was used to do fluorescence recovery after photobleaching (FRAP) analysis of wild type Gal4-GFP in the nuclei of live cells. The above microscopy was performed as described in Figure 3 using a 488nm laser for excitation and a 505-530BP filter for detection. The representative time lapse series shown in (**A**) and (**B**) are examples of images captured of Gal4-GFP in *WT* cells. The above 'pre' frame represents the total fluorescent signal prior to bleaching. The 'post' frame is the scan immediately following the bleach event. Subsequent images are points taken every second thereafter under inducing (SC+Gal; **A**) and uninducing conditions (SC+Raf; **B**), respectively. (**C**) Wild type Gal4-GFP in *GAL80* (*WT*) cells is diffusionally constrained in inducing (SC+Gal) media but not in uninducing (SC+Raf) media. (**E**) Values for $t_{1/2}$ of association were calculated from FRAP data showin in (**C**) and (**D**) by using GraphPad Prism software.

the shuttling function, and that both Gal4 and its target genes are mutually dependent partners in perinuclear anchoring. If so, tethering of Gal4 to the nuclear periphery should

require its DNA-binding domain. We therefore tested GFP-tagged Gal4 (Δ1-50), designated ΔDBD (Figure 18A), in the FRAP and NPC co-fractionation assays. The results indicated that Gal4 does not require its DNA binding domain, either to co-fractionate with NPCs (Figure 19A) or to undergo slower diffusion in the presence of galactose (Figure 19B). These data suggest that peripheral anchoring of Gal4 occurs independently of its target genes.

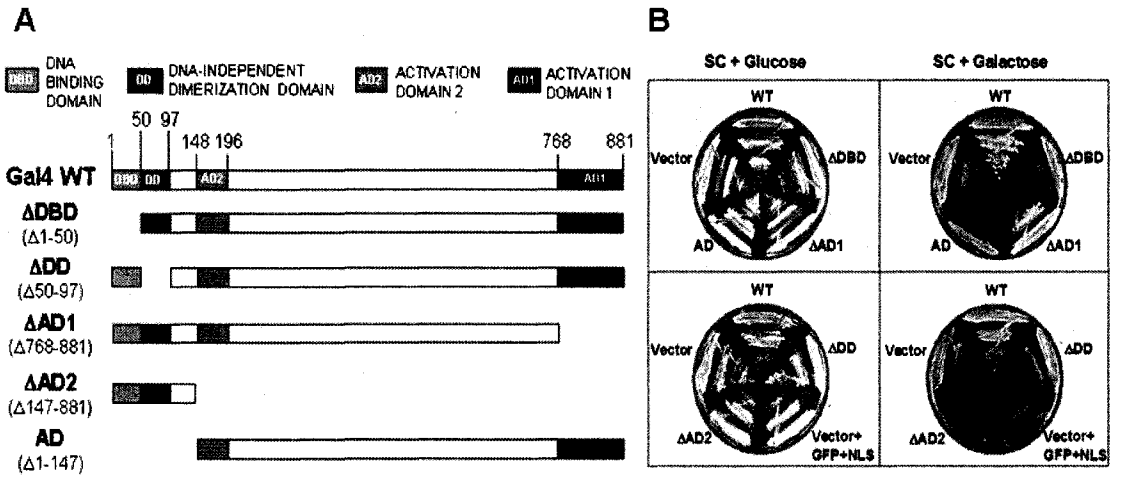

Figure 18. Gal4 derivatives missing one or more key domains. (**A**) Each diagram (ΔDBD, ΔDD, ΔAD1, ΔAD2, AD) depicts the residues that remain present in the corresponding Gal4 derivative. Each of these derivatives contains the SV40 NLS and a GFP tag at the C-terminus (not shown). (**B**) Each derivative from (**A**) was introduced into *Δgal4* cells to test complementation of impaired growth on galactose. Synthetic complete (SC) agar was supplemented with either glucose or galactose as indicated. Pictures were taken after 72h at 30C.

We wondered what if any role the other well-established domains of Gal4, the dimerization domain and the activation domains (Figure 2), might play in the galactose-induced, DNA-independent perinuclear anchoring of Gal4. We therefore tested fluorescently tagged, mutated Gal4 derivatives lacking each of these domains; Western blot analysis and fluorescence quantitation indicated that expression of each C-terminally tagged GFP variant depicted in Figure 18A is roughly equivalent to wild type Gal4-GFP.

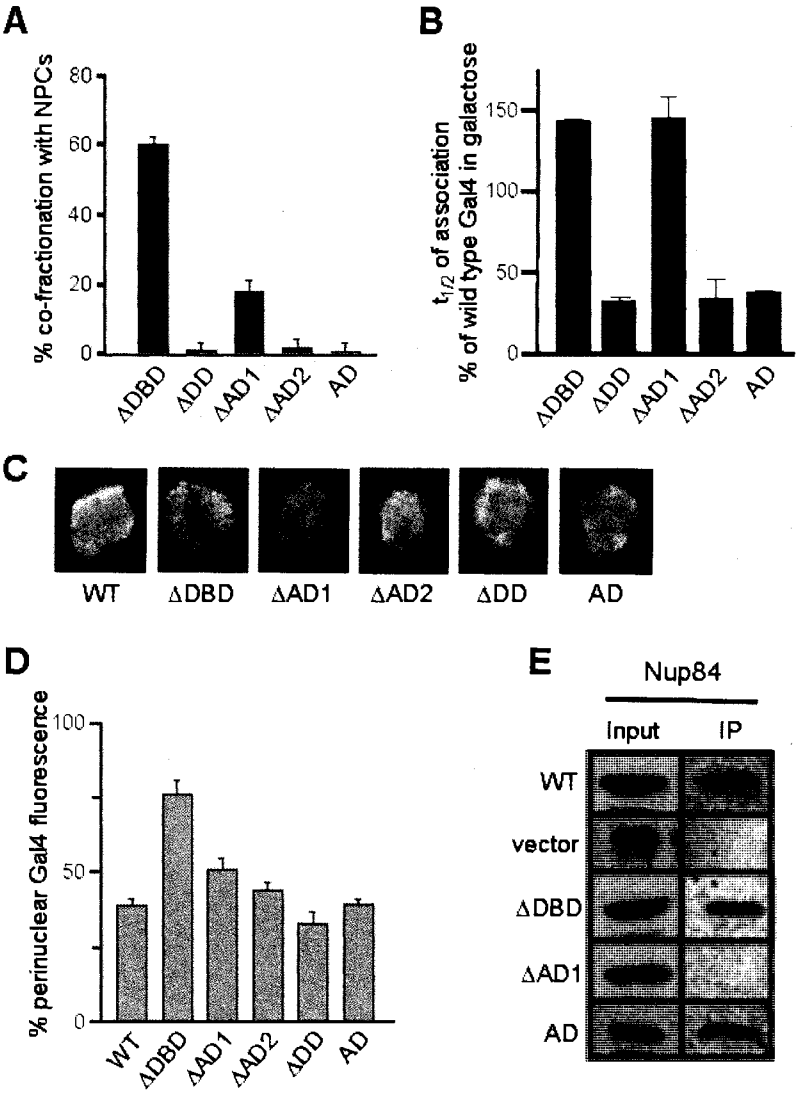

Figure 19. Interaction between Gal4 and perinuclear factors. Wild type Gal4 and deletion derivatives, tagged with GFP and NLS moieties (see Figure 18A) were moderately overexpressed from a multicopy plasmid: DNA binding domain removed (DDBD), primary activation domain removed (DAD1), both activation domains removed (DAD2), dimerization domain removed (DDD), both DBD and DD removed (AD). (**A**) Cells expressing deletion derivatives of wild type *GAL4* were grown in inducing (SC+Gal) media; co-fractionation with NPCs was determined for the corresponding products: DDBD, DDD, DAD1, DAD2 and AD (see Figure 18A).(**B**) A Zeiss confocal laser-scanning microscope was used to do fluorescence recovery after photobleaching (FRAP) analysis of mutated Gal4-GFP in the nuclei of live cells. Values for t1/2 of association were calculated for deletion derivatives of Gal4-GFP in cells grown in inducing (SC+Gal) media. (**C**) Plasmids were introduced into a strain harboring chromosomal *NUP49*-tDimer2 and *NUP60*-tDimer2 alleles; representative merged GFP+tDimer2 CLSM images of mid-log galactose-grown cells are shown for each transformant. Quantitation (see text) indicated that these GFP variants were expressed at equivalent

steady-state levels; (**D**) Perinuclear Gal4-GFP fluorescence is defined for each transformant as the percentage of total GFP fluorescence that is localized to the outer one-third of the nuclear area; note that a value of 33% is equivalent to a random distribution. (**E**) Plasmids were introduced into a strain harboring a gene encoding epitope-tagged Nup84; a-GFP antibody was used to immunoprecipitate Gal4-GFP from extracts of each transformant. Western blot shows co-immunoprecipitation of Nup84 (IP) relative to input levels. Vector, transformant containing empty multicopy plasmid.

Since Gal4 is required for growth in galactose, each mutant can be tested for function by complementation analysis in *Δgal4* cells. Cells lacking native Gal4, expressing plasmid borne Gal4 variants were grown on selective SC media supplemented with either 2% glucose or 3% galactose for 72 hours at 30°C. Impairment of growth on galactose (Figure 18B) upon deletion of Gal4DD (the ΔDD mutant), Gal4AD1 (the ΔAD1 mutant), or combined deletion of both activation domains (the ΔAD2 mutant), is consistent with the classical analysis of mutations in Gal4 (Ma and Ptashne 1987). As expected, ΔAD1 cells are only partially defective (Figure 18B) due to the presence of the second, weaker activation domain. Strikingly, in galactose-grown cells there is a correlation between impairment of growth and co-fractionation of Gal4 with NPCs. The removal of DD (ΔDD or AD), or removal of both ADs (ΔAD2), eliminated Gal4 from perinuclear fractions (Figure 19A) though it remained in the nucleus (Figure 19C). These data suggest that a functional DD and AD are essential for galactose-dependent perinuclear co-fractionation of Gal4 with the NPC.

FRAP analysis confirmed the conclusions drawn from perinuclear co-fractionation data; Gal4 derivatives that lacked either the dimerization domain (the ΔDD and AD mutants; Figure 18A), or both activation domains (the ΔAD2 mutant), failed to exhibit *in vivo* structural association in the nuclei of galactose-grown cells (Figure 19B). We noted

that the Gal4 derivatives lacking either the DNA binding domain (ΔDBD) or the primary activation domain (ΔAD1) exhibited even greater diffusional constraint than wild type Gal4; this might be a consequence of eliminating the myriad of non-specific interactions mediated by Gal4DBD and Gal4AD, respectively (see below). Overall the data in Figure 19 indicate an important role for the dimerization and activation domains, but not the DNA binding domain, in perinuclear anchoring of the Gal4 activator.

While doing FRAP analysis we noticed that the nuclear distribution of ΔDBD differed from wild type and also differed from the other Gal4 derivatives lacking one or more key domains; ΔDBD exhibited a distinct perinuclear pattern (Figure 19C). This does not result from a nuclear import defect, since each Gal4 derivative contains an identical, well-characterized NLS (Figure 18A). We verified the perinuclear localization of the ΔDBD derivative by using the Zeiss LSM510 imaging software to quantitate the distribution of fluorescent Gal4 molecules in the nuclei of live cells (Figure 19D). These data suggest that perinuclear localization of Gal4 is normally blurred by its DNA binding domain; presumably this is a consequence of the multitude of non-specific binding interactions between Gal4DBD and the large amount of chromatin that is distributed throughout the yeast nucleoplasm. These weak interactions might also explain the greater mobility of wild type Gal4 relative to ΔDBD that was detected by FRAP analysis of galactose-grown cells (Figures 17E & 19B). A similar phenomenon presumably explains the FRAP result for ΔAD1, since the capacity of the primary Gal4 AD to undergo promiscuous weak interactions with a variety of targets (Melcher 2000) might serve to increase the overall mobility of wild type Gal4.

Further confirmation of perinuclear tethering was obtained by testing for a physical interaction with co-immunoprecipitation between Gal4 and components of the NPC. We found a robust interaction between Gal4 and Nup84 (Figure 19E), the eponymous subunit of the Nup84 subcomplex that mediates transcriptional induction of both Rap1/Gcr1 and Snf1/Mig1 targets (Menon *et al.* 2005; Santangelo 2006; Sarma *et al.* 2007). Interestingly, Gal4AD1 is required for this interaction, whereas Gal4DBD and Gal4DD are dispensable (Figure 19E; note that the AD mutant=ΔDBD+ΔDD; see Figure 18A). Though we do not fully understand the details of this interaction, it does provide compelling evidence that Gal4 may play a significant role at the nuclear periphery.

CHAPTER VII

DISCUSSION

This work suggests that the function of classically described positively and negatively acting regulators can be explained by their movement into and out of the perinuclear compartment and that the transcriptional regulation of genes occurs as a consequence of translocation to the nuclear periphery. This is consistent with the previously proposed reverse recruitment model of gene regulation (Menon *et al.* 2005). Further, this and previous work demonstrates that the NPC, in particular the Nup84 subcomplex, plays an important role in transcriptional regulation of at least two classes of glucose-regulated genes, Rap1/Gcr1 and Snf1/Mig1 targets (Menon *et al.* 2005; Sarma *et al.* 2007) as well as the galactose-induced Gal4 targets. A connection between transcriptional activity and the nuclear periphery can be observed directly by tagging NPC-regulated genes with green fluorescent protein (GFP). Insertion of an array of *lac* operators at a single chromosomal site, in cells that express LacI-GFP, results in the appearance of a bright green spot in the nucleus. This spot marks the position of loci that are tightly linked to the lac_{op} array (see above). The *in vivo* subnuclear position of such GFP-tagged genes can be monitored within a confocal optical slice of the nucleus. Several labs including ours have used this technique to observe regulated yeast genes moving to, and becoming anchored at, the nuclear periphery when they are transcriptionally active (Brickner *et al.* 2007; Casolari *et al.* 2004; Sarma *et al.* 2007; Taddei *et al.* 2006).

Glucose Regulation of *SUC2* Occurs at the Nuclear Periphery

To examine glucose repression we used the well-studied invertase encoding gene *SUC2*. In order to elucidate possible connections between gene localization and expression we took a closer look at the relevant regulators. Expression of *SUC2* is inhibited through a collaboration of DNA-bound Mig1, Hxk2 and the Ssn6/Tup1 complex. I show here that the Mig1 repressor is present in the perinuclear compartment and bound to the *SUC2* promoter only in the presence of glucose (Figure 8C & 9B), its co-repressor Ssn6 is also perinuclear and bound to *SUC2* during repression (Figure 8C; Sarma *et al.* 2007). Conversely, in the absence of glucose Mig1 is phosophorylated by the Snf1 kinase complex and evicted from the nucleus. This phosphorylation of Mig1 may also occur at the nuclear periphery where we see an enrichment of Snf1 (Sarma *et al.* 2007). Importantly, it appears that removing Hxk2 from cells causes a defect in glucose repression of *SUC2* at least in part, by causing Mig1 to be unable to localize the nuclear periphery. Derepression caused by this failure of Mig1 to become peripheral is equivalent to removing Mig1 from cells altogether (Table 3; Figure 9B). This suggests that the nuclear periphery is a host to a number of regulatory actions which facilitates both active expression and repression.

The presence and proposed significance of these regulators at the nuclear periphery provides some explanation for our previously observed glucose dependent nucleoporin activation (Menon *et al.* 2005; Sarma *et al.* 2007). In our previous reports, we have found that glucose regulation is deranged upon removal of structurally immobile perinuclear factors. For example, in *Δnup133* cells *SUC2* expression, as measured by invertase activity, is at least twofold reduced, as compared to *WT* cells, in the absence of glucose. Likewise, in the presence of glucose, *SUC2* expression is approximately fivefold

derepressed again compared to *WT* cells (Sarma and Santangelo; our unpublished data). We observe these changes in regulation despite normal nucleocytoplasmic shuttling of Mig1 and Snf1 in *Δnup133* cells (Sarma 2007; Sarma *et al.* 2007). Taken together, these data suggest that regulation of glucose-repressed yeast genes takes place at the nuclear periphery and further suggest that the Nup84 subcomplex, an essential structure within NPCs, plays a critical role.

Consistent with the perinuclear location of its regulators (Mig1, Ssn6, and Snf1), as well as the loss of glucose derepression in the absence of genes encoding perinuclear factors, *SUC2* is tightly constrained the periphery when active and exhibits greatly increased mobility when repressed (Figure 8A, B). However, despite the increased mobility during repressing conditions, a physical interaction between *SUC2* and NPCs can still be detected using ChIP (Figure 8C). One simple explanation for this result might be that a transient random interaction is sufficient to produce a strong ChIP signal; alternatively, the gene may periodically revisit the site of regulatory action in the perinuclear compartment. We favor the latter explanation, that the repressed *SUC2* gene occasionally makes physical contact with one or more perinuclear sites of activation but is unable to establish a productive interaction due to Hxk2-mediated interference by the perinuclear Mig1/ Ssn6 repressor. Additionally, the *SUC2* ORF was found at the nuclear periphery in 45% of wild-type cells under repressing conditions. This is significantly above the 33.3% expected by chance, indicating that the distribution of the gene under these conditions is not random.

The above suggests that the glucose-repressed *SUC2* gene will localize to the nuclear periphery periodically, perhaps by random motion. The determining factor for

peripheral constraint and subsequent expression rests with the regulatory elements the gene comes into contact with proximal to the NPC. This behavior is consistent with a reverse recruitment model of gene regulation (Figure 1B). Though this work adds significant insight into glucose regulation of *SUC2* at the nuclear periphery, much remains to be discovered in the details of gene constraint for activation and the role Mig1 plays at the periphery.

GAL Genes Move to the Nuclear Periphery Prior to Expression

Like *SUC2*, induction of *GAL1* gene expression has effects on its subnuclear gene localization. Using the GFP gene tagging technique (see above) we observed the movement of the *GAL* genes to the nuclear periphery upon galactose induction (Figure 10B). This relocalization of *GAL1* has been observed previously via cell biology in both fixed (Casolari *et al.* 2004) and live cells (Drubin *et al.* 2006). By utilizing ChIP analysis as described above, we found that components of the Nup84 subcomplex constitutively interact with the promoter region of *GAL1* (i.e. in both induced and uninduced conditions; Sarma and Santangelo; our unpublished data). This result is reminiscent of the interaction we observed for *SUC2* (see above), suggesting that this gene-NPC interfacing may be a common feature of gene regulation.

In this study we have added a new component to GFP-gene tracking system for the *GAL* genes, by adding the ability to monitor expression. In replacing *GAL1* with fluorescent *GFP-RAS2*, it is possible to simultaneously visualize the *GAL* genes nuclear location coordinately with expression (Figures 12A & B). This modified assay to track gene location served to address an important question. Does gene relocation to the periphery occur prior to expression of the product? This does indeed appear to be the case

as we saw an increase in perinuclear *GAL1* expressors, in this case represented by GFP-Ras2, prior to the appearance of nucleoplasmic *GAL1* expressors (Figure 13B & C). This strongly suggests that perinuclear localization of the gene occurs prior to its expression. Interestingly, we also found that the fraction of nucleoplasmic expressors peak at ninety minutes, suggesting that if *GAL* genes are exclusively activated at the nuclear periphery, they can be temporarily released to the nucleoplasm (Figure 13B). Though this aspect has not been explored directly, one idea is that this may be related to an oscillatory progression of expression following gene induction that we have previously observed in transcriptomic analyses (Barbara and Santangelo; our unpublished data). As cells respond to a transcriptomic signal, a high spike in target gene expression could be followed by attenuation through feedback in the signal, releasing the gene from the periphery.
Our observations in the timing of expression are consistent with what has been reported by Brickner *et al.* who examined the timing of *GAL1* and *INO1* expression, using RT-PCR, following induction. Since we observe that the gene relocates to nuclear periphery prior to the detection of expression, this makes an additional supporting argument for reverse recruitment. However, neither RT-PCR nor our *GFP-RAS2* reporter strain is sufficient to completely rule out the possibility that a "pioneer round" (see Background and Significance) of transcription precedes gene movement to the nuclear periphery. Since chromophore maturation (this work) and the sensitivity of RT-PCR (Brickner *et al.* 2007) require an accumulation of transcript product, these limitations must be taken into account.

We attempted to address this issue by observing the mobility and localization of the *GAL1* gene when induced by galactose during a transcriptional block. To accomplish

this we added the *GAL1* GFP-gene tracking system into cells expressing only the temperature sensitive allele of the Pol II large subunit (*rpb1-1*). If the *GAL1* gene relocates to the nuclear periphery following galactose induction in *rpb1-1* cells held at the non-permissive temperature (Nonet *et al.* 1987), then transcriptional activity is most likely not a prerequisite for perinuclear localization. This is exactly what we observed (Figure 14). Interestingly, we can maintain the anchored *GAL1* gene with the transcriptional block for at least four hours without detriment to the cell (Figure 14D). However, only after addition of galactose and being shifted to the permissive temperature do we see the gene constrained to the nuclear periphery and detect the gene product (Figure 14E). Similar evidence using the *rpb1-1* allele has been reported for *INO1* (Brickner *et al.* 2007).

These data provide further insight into the reverse recruitment mechanism on the part of timing. Genes relocating to the nuclear periphery prior to expression is consistent with this model of regulation. What these data do not rule out is the possibility that a partially transcribed product may be produced even at the non-permissive temperature and that this initial portion of the mRNA product is sufficient for movement to the periphery. Since the exact nature of transcriptional shutoff imposed by the *rpb1-1* allele is unknown, further work will still need to be done to determine once and for all the sequence of events that leads to gene movement to the nuclear periphery.

Components of the Pre-initiation Complex at the Nuclear Periphery

Taken together the above data suggest that perinuclear anchoring prior to transcription initiation/elongation may be a common feature of yeast gene induction. If this is true, it is likely that components of the transcriptional machinery, in particular Pol

II itself, should exhibit both functional and physical association with NPCs and other perinuclear factors. Evidence for a functional link includes the observation that activator bypass, for example by the Mediator subunit Ssn8/Srb11, is impaired by removal of Nup84 complex subunits and the perinuclear transcription factor Gcr1 (Menon *et al.* 2005). Also, transcriptional regulation at many loci—e.g. *SUC2*, other glucose-repressed genes, Rap1/Gcr1 targets and *GAL* genes—is impaired by the removal of NPC subunits. For each of these systems we have found that the regulatory defects are independent of the NPC role in nuclear import/export (Menon *et al.* 2005; Santangelo 2006; Sarma *et al.* 2007; our unpublished data). Further, we have previously reported that a number of nucleoporins are able to activate transcription of a reporter gene when fused to a DNA-binding domain (Menon *et al.* 2005).

A physical link between yeast Pol II and NPCs was first suggested by a large body of proteomic data (Menon *et al.* 2005). In this study, we attempted to co-fractionate components of the Mediator, TFIID and Pol II complex with the integral membrane protein Pom152. Interestingly, all factors tested were found to co-fractionate with the NPC (Figure 15A) and this localization was independent of carbon source (Sarma and Santangelo; our unpublished data). This co-fractionation we observed could have been due to these factors being associated with active genes found at the nuclear periphery. However, this scenario is unlikely as a DNAse step is used in the process of fractionation. Considering that this DNA-independent peripheral localization could be intrinsic to active transcription, we repeated the fractionation in *rpb1-1* cells under transcriptional shutoff (Figure 15B). After four hours at the non-permissive temperature we were still able to detect these factors at the nuclear periphery.

These data contribute another piece of the puzzle facing the regulation of genes at the periphery. According to our observations, components of the transcriptional machinery do in fact localize to the nuclear periphery and this localization occurs in the absence of transcription. This allows us to make a more firm statement regarding the "pioneer round" of transcription preceding gene movement to the periphery. If the "pioneer round" of expression occurred prior to peripheral gene localization that would postulate that these transcription factors are tethered to the nuclear periphery in a DNA dependent fashion. However, as mentioned above, these factors are retained to the periphery in both the absence of DNA association (Figure 15A) and active transcription (Figure 15B). This implies that at least some components of the transcription machinery are localized to the nuclear periphery at all times.

Gal4 Contacts its Target Genes and NPCs When Active

With the data presented here with previous reports, it is clear that the *GAL* genes likely move to the nuclear periphery in order to become active. The *GFP-RAS2* reporter assay showed that genes at the nuclear periphery start to express the gene product sooner after galactose induction than genes that reside in the nucleoplasm. Additionally, we've shown that the *GAL* genes can relocate to the periphery in response to galactose, even during a transcriptional block. Since we observe components of the transcriptional machinery in the perinuclear compartment, regardless of transcriptional state, it stands to reason that the genes are moving to the nuclear periphery to contact the transcriptional machinery, along with other factors, and become active. The question then remains, what role do the transcriptional regulators (i.e. the activator Gal4, and the repressor Gal80) play in this process?

It was previously reported that in order to detect an interaction between NPCs and the promoter of *GAL1*, cells required a functional Gal4 (Schmid *et al.* 2006). Consistent with this report, we show here that in the absence of Gal4, the *GAL1* gene fails to become constrained and remains highly mobile in inducing conditions (Figure 7B). It is unclear exactly what effect removing Gal4 actually has on *GAL1* and its inability to interact with the nuclear periphery. A couple of possibilities include but are not limited to: Gal4 is a tethering factor that functions in *GAL1* retention to the periphery or Gal4 is involved in the shuttling of *GAL1* to the periphery for activation. Conversely, in the absence of the repressor Gal80, *GAL1* becomes constitutively perinuclear (Figure 7B). These data demonstrate that localization of *GAL* genes to the nuclear periphery is governed by the normal Gal4/Gal80 regulatory mechanism.

In order to examine the possibility that Gal4 assists in anchoring the *GAL* genes to the periphery for activation, we attempted to co-fractionate Gal4 with the NPC. We found that Gal4 co-fractionates with the NPC only in galactose, clearly exhibiting an inducible functional link to the nuclear periphery (Figure 16). We further show that in galactose Gal4 interacts physically with the essential Nup84 subcomplex via co-immunoprecipitation (Figure 19E). This interaction likely explains the reduction in Gal4 mobility seen by performing either iFRAP or FRAP analyses (Figure 7F &17C). By removal of the Gal4 inhibitor Gal80, this peripheral localization and slower form of Gal4 becomes constitutive (Figure 16 & 17D). These data suggest that Gal4, like its target genes, anchors at NPCs upon galactose induction. Since Gal4 is found to be contacting its promoter sequence constitutively, Gal80 appears to inhibit expression of the *GAL* genes by preventing Gal4 from interacting with the nuclear periphery through an alternate

contact surface. This provides some evidence that Gal4 facilitates the anchoring of its target genes to the nuclear periphery for activation.

The above observations seemingly place Gal4 as the common factor shared by active *GAL1* and the NPC. Since Gal4 has been characterized into well characterized modular domains, it was likely one or more of these domains common to transcriptional activators may participate in these separate interactions (i.e. DNA-binding and peripheral tethering). We therefore undertook an analysis of domain deletion mutants to examine each known functional domain of Gal4. First, we examined the DNA binding domain and found that its absence was irrelevant to Gal4 peripheral co-fractionation (Figure 19A), interaction with Nup84 (Figure 19E) or its mobility (Figure 19B). Therefore, galactose-dependent anchoring of the Gal4 activator at the nuclear periphery is independent of its interaction with DNA. This result is consistent with our hypothesis of Gal80 inhibition through a separate contact surface. Interestingly, we observed that in the absence of the Gal4 DBD, distribution of the protein was mostly punctate and perinuclear (Figures 19C & D) as opposed to the wild type distribution, in which the punctuate foci are less constrained to the nuclear periphery. The difference is most likely the result of non-specific DNA-binding interactions between Gal4 and nuclear DNA (see Background).

Further mutational analysis explored the remaining domains of Gal4 (Figure 18A). Removal of the dimerization domain or both activation domains eliminates Gal4 from the nuclear periphery (Figure 19A). This was recapitulated by the FRAP experiments, which illustrated that deletion of the dimerization domain or both activation domains resulted in the failure of Gal4 to shift to a slower-diffusing form upon inducing conditions (Figure 19B). This indicated that the galactose-dependent perinuclear co-

fractionation of Gal4 requires both a functional dimerization domain and a functional activation domain. Interestingly, removal of the primary activation domain was sufficient to cause a loss of Gal4 interaction with Nup84 (Figure 19E). Despite this loss of contact, Gal4-ΔAD1 remains at the nuclear periphery and is able to partially compliment cells grown on galactose (Figure 19A & 18B). This observation suggests that the secondary, weaker activation domain is still able to contact perinuclear factors for activation of its target genes.

From these data we can postulate distinct contributions of the dimerization domain and primary activation domain in Gal4. The Gal4 dimerization domain (DD) is required for anchoring interaction(s) with one or more nuclear structures as shown with co-fractionation and FRAP, however it is dispensable for a physical interaction with the Nup84 subcomplex; the reverse is true for the Gal4 primary activation domain (AD1; Figures 19A, B & E).

All of these data expanding on what is known about the domains of Gal4 in the context of perinuclear gene activation are consistent with a straightforward reverse recruitment model (Figure 20). In uninducing conditions, Gal80 interacts DNA-bound Gal4, preventing productive contact with the nuclear periphery, thus inhibiting *GAL* gene expression. In cells exposed to galactose, Gal80 is sequestered away from Gal4 into the cytoplasm, freeing the contact surface required for peripheral association. This allows the DNA-bound Gal4 dimer to interact with components at the NPC, tethering its target genes to the nuclear periphery which facilitates transcriptional activation.

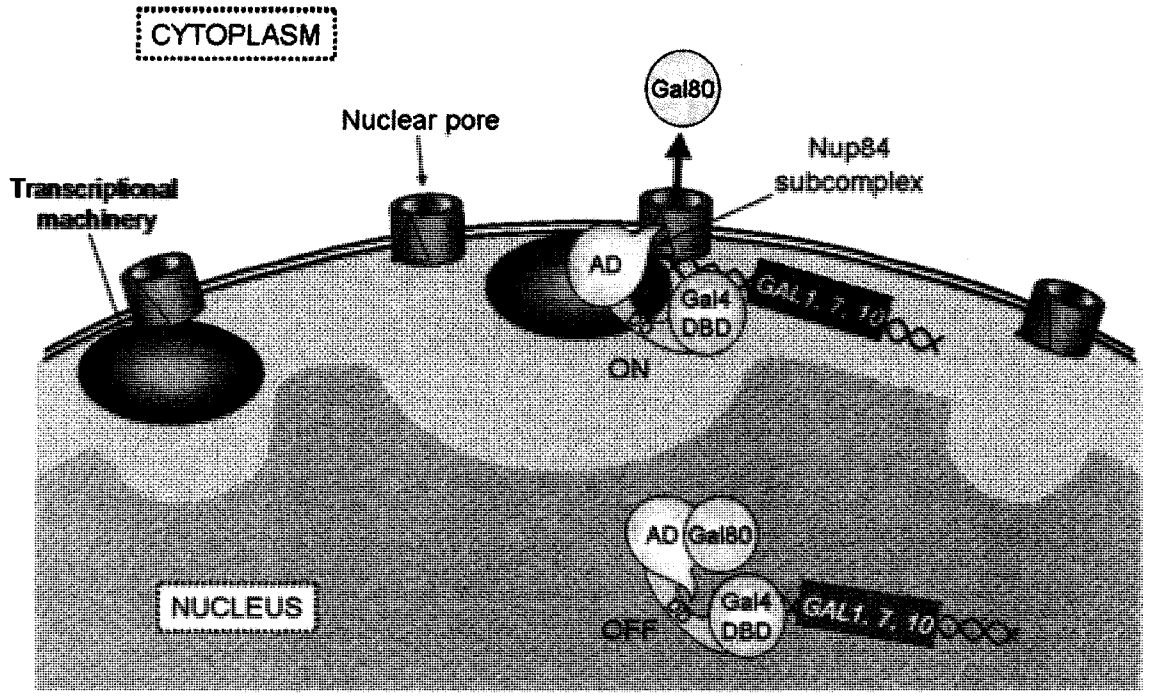

Figure 20. GAL gene expression occurs via a reverse recruitment mechanism. When transcription of the *GAL* genes is OFF, they reside primarily in the nucleoplasm; Gal4 may bind DNA in the uninduced state but a productive interaction with the transcriptional machinery is prevented by the Gal80 repressor, which masks the Gal4AD. When the genes are induced by galactose (ON), Gal80 dissociates and is exported to the cytoplasm. The Gal4AD then interacts with the transcriptional machinery at the nuclear periphery and the *GAL* genes are expressed.

Gene Movement by Chromatin Remodeling

It is tempting to conclude that transcriptional activators simply bridge their target genes with the perinuclear transcriptional machinery. However, there are many known levels of gene regulation which may also contribute to such a 3D model. Another such input into gene translocation to the perinuclear compartment, involves the well characterized correlation between euchromatin and active genes. The process of chromatin remodeling through histone acetylation and nucleosomal rearrangement is a conserved feature in most organisms (Bendich and Drlica 2000). Though many exceptions have been identified, the current view of chromosome architecture is that hyper-acetylated histones or chromatin regions depleted of nucleosomes mark a locus as

transcriptionally active. Conversely, tightly compacted chromatin comprised of hypo-acetylated histones and nucleosome dense regions indicate silenced loci (Figure 21A). A handful of complexes that are largely conserved in eukaryotes are attributed to this action of chromatin conversion.

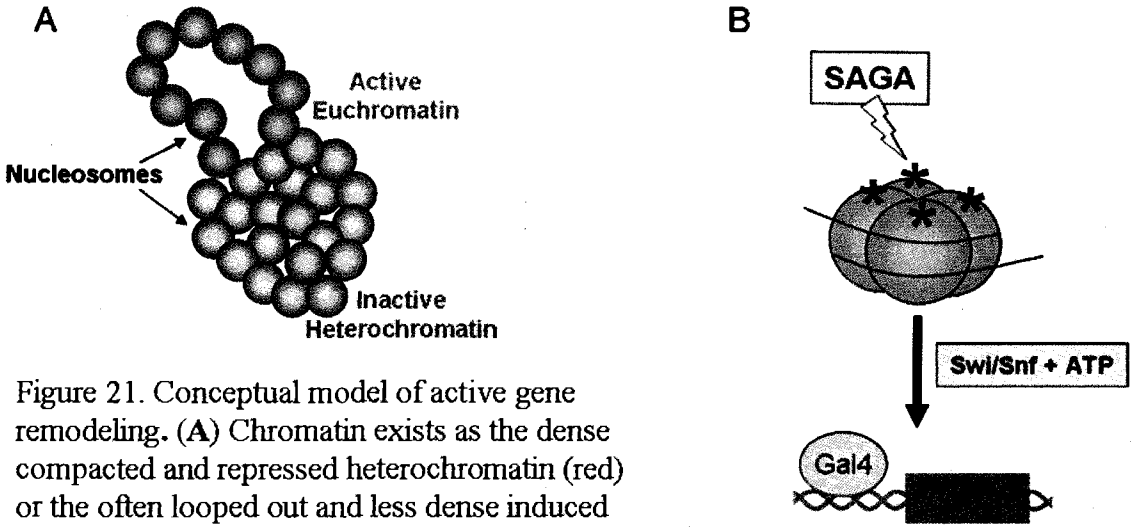

Figure 21. Conceptual model of active gene remodeling. (**A**) Chromatin exists as the dense compacted and repressed heterochromatin (red) or the often looped out and less dense induced euchromatin (blue). (**B**) When the gene is induced, nearby histones are acetylated by SAGA (or another histone acetyltransferase complex) and the local chromatin is remodeled by the Swi/Snf ATP-dependent complex. Finally, the DNA-bound activator and gene can establish a productive interaction with the transcriptional machinery at the nuclear periphery.

In *S. cerevisiae*, histone acetylation is accomplished, in part, by the Gcn5 transacetylase subunit of the SAGA complex. Through Sgf73, SAGA associates with the target promoter and acetylates the histone 2B subunits of the local histones (Chandy *et al.* 2006) converting the region to a less dense euchromatin state. Following the acetylation of histones by SAGA, the ATP dependent Swi/Snf complex contacts the region and translocates or evicts proximal nucleosomes (Chandy *et al.* 2006). This action is postulated to mark the gene for activation (Figure 21B). The unanswered question remains, how does the active gene mobilize to the nuclear periphery?

In order to address this question, it's important to consider the inactive heterochromatin. An *in vitro* study found that heterochromatin will accumulate intrinsically and is sufficient to repress transcription (Tse *et al.* 1998). Our data suggest that Htb2 exists within a largely immobile population within the nucleus (Figure 7B); consistent with the notion that chromatin defaults to a transcriptionally silent state. Energetically, this makes sense since remodeling by the Swi/Snf complex for activation requires energy in the form of ATP. If we assume that highly condensed heterochromatin accounts for the majority of the unexpressed portion of the genome, we can speculate a model for gene movement to the periphery based on the architectural dichotomy of hetero- and euchromatin.

This model postulates that remodeling will create a chromatin "loop" of lower density that will conflict with the surrounding compacted heterochromatin; resulting in an innate relocalization of the gene to less dense regions of the nucleus (Figure 22). This work and reports from many other labs have shown that the destination of induced genes is the nuclear periphery, specifically the NPC. The question remains, what targets the NPC as a destination for remodeled promoters? The answer again may lie within the inactive heterochromatin. It can be theorized that the heterochromatin creates a network of subnuclear architecture arranged as a dense central core with extending regions of silent chromatin that contact the nuclear periphery in the space between NPCs (Figure 22; Taddei *et al.* 2004). These regions of perinuclear silent chromatin are conserved in higher eukaryotes (Chambeyron and Bickmore 2004).

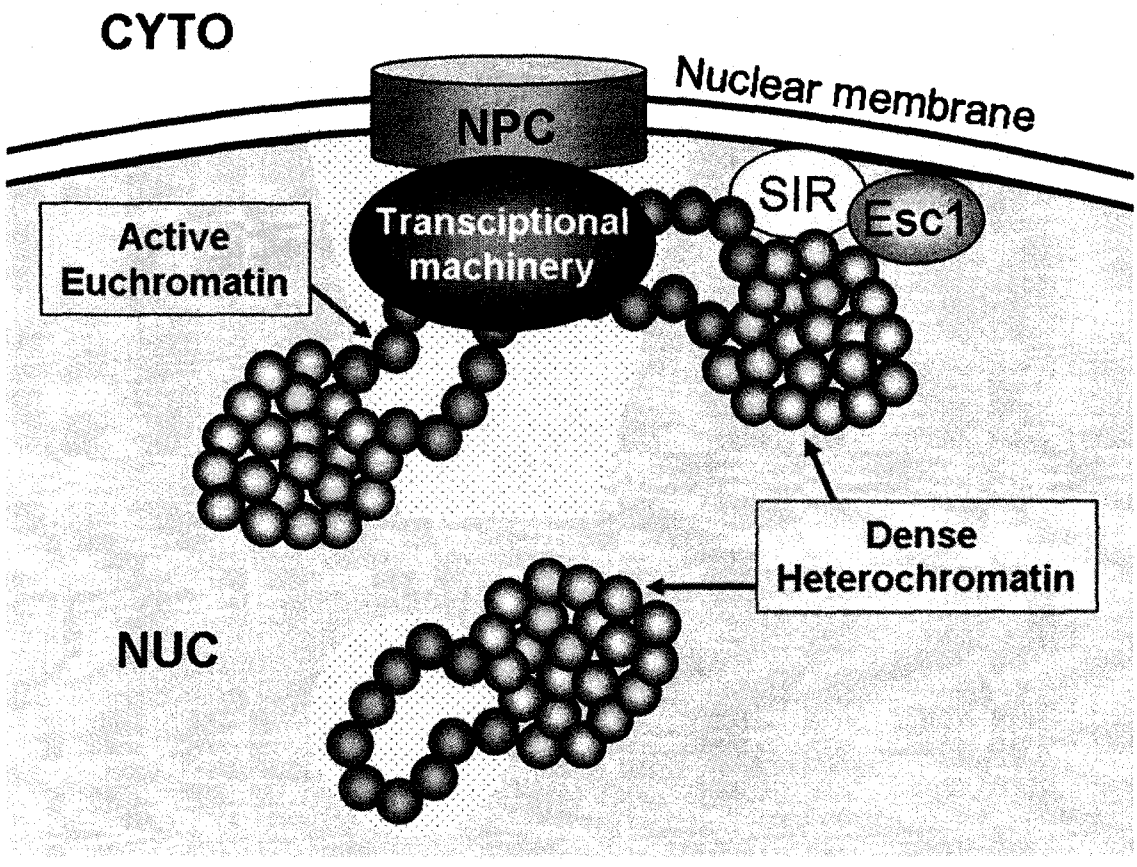

Figure 22. The difference in density between active and inactive chromatin could be an organizational feature of gene expression. Tightly packaged heterochromatin (red) is dense; active euchromatin (blue) is less dense and often 'looped out'. This can create bubbles of low density (white speckled area) within the densely packed nucleus (light red). Bubbles can aggregate into a low density pocket at the nuclear pore complex (NPC) to contact the transcriptional machinery that resides there. Adjacent heterochromatin can still contact silencing factors, such as the SIR proteins and Esc1, which reside at the periphery between NPCs and help to establish long-term gene silencing.

Once an active gene reaches the NPC, the promoter is able to interact with the NPC components as well as the general transcription machinery and transcriptional activation can commence. Recent work has suggested that further remodeling of active genes can occur with the incorporation of the histone 2A variant H2A.Z, encoded by Htz1 in yeast, for the purpose of transcriptional memory (Brickner *et al.* 2007). Memory postulates that recently transcribed genes whose activating signal is depleted are able to

reinitiate transcription more quickly. It's been shown that H2A.Z mimics properties of hyper-acetylation and is resistant to nucleosomal condensation (Fan *et al.* 2002). Thus, the incorporation of H2A.Z may also contribute to the peripheral constraint observed for active genes.

Additional to this work, there are several questions that I'd like to see answered: (A) Where does the 'pioneer round' of transcription occur in the nucleus? (B) What are the specific contact points between Gal4 and peripheral factors? (C) Using rpb1-1 cells also containing temperature sensitive chromatin remodeling factors; do the *GAL* genes still localize to the nuclear periphery at the non-permissive temperature when exposed to galactose?

Though much remains to be done in elucidating the mechanistic details and order of events, it is clear that transcriptional regulators and chromatin architecture play a role in gene movement to the nuclear periphery. Since the *GAL* regulatory system and the Gal4 activator in particular were used to establish the original paradigm for gene regulation, together, my work suggests that the reverse recruitment model (Menon *et al.* 2005) may explain how transcriptional activation works in many eukaryotic regulatory systems.

REFERENCES

Akhtar A, Gasser SM. 2007. The nuclear envelope and transcriptional control. Nat Rev Genet 8(7):507-17.

Balciunas D, Hallberg M, Bjorklund S, Ronne H. 2003. Functional interactions within yeast mediator and evidence of differential subunit modifications. J Biol Chem 278(6):3831-9.

Barberis A, Pearlberg J, Simkovich N, Farrell S, Reinagel P, Bamdad C, Sigal G, Ptashne M. 1995. Contact with a component of the polymerase II holoenzyme suffices for gene activation. Cell 81(3):359-68.

Bendich AJ, Drlica K. 2000. Prokaryotic and eukaryotic chromosomes: what's the difference? Bioessays 22(5):481-6.

Blobel G. 1985. Gene gating: a hypothesis. Proc Natl Acad Sci U S A 82(24):8527-9.

Boe SO, Haave M, Jul-Larsen A, Grudic A, Bjerkvig R, Lonning PE. 2006. Promyelocytic leukemia nuclear bodies are predetermined processing sites for damaged DNA. J Cell Sci 119(Pt 16):3284-95.

Brand M, Leurent C, Mallouh V, Tora L, Schultz P. 1999. Three-dimensional structures of the TAFII-containing complexes TFIID and TFTC. Science 286(5447):2151-3.

Brickner DG, Cajigas I, Fondufe-Mittendorf Y, Ahmed S, Lee PC, Widom J, Brickner JH. 2007. H2A.Z-mediated localization of genes at the nuclear periphery confers epigenetic memory of previous transcriptional state. PLoS Biol 5(4):e81.

Brickner JH, Walter P. 2004. Gene recruitment of the activated INO1 locus to the nuclear membrane. PLoS Biol 2(11):e342.

Brown CR, Silver PA. 2007. Transcriptional regulation at the nuclear pore complex. Curr Opin Genet Dev 17(2):100-6.

Brown T, Mackey K, Du T. 2004. Analysis of RNA by northern and slot blot hybridization. Curr Protoc Mol Biol Chapter 4:Unit 4 9.

Cabal GG, Genovesio A, Rodriguez-Navarro S, Zimmer C, Gadal O, Lesne A, Buc H, Feuerbach-Fournier F, Olivo-Marin JC, Hurt EC and others. 2006. SAGA interacting factors confine sub-diffusion of transcribed genes to the nuclear envelope. Nature 441(7094):770-3.

Carey M, Kakidani H, Leatherwood J, Mostashari F, Ptashne M. 1989. An amino-terminal fragment of GAL4 binds DNA as a dimer. J Mol Biol 209(3):423-32.

Carlson M. 1999. Glucose repression in yeast. Curr Opin Microbiol 2(2):202-7.

Casolari JM, Brown CR, Komili S, West J, Hieronymus H, Silver PA. 2004. Genome-wide localization of the nuclear transport machinery couples transcriptional status and nuclear organization. Cell 117(4):427-39.

Chambeyron S, Bickmore WA. 2004. Chromatin decondensation and nuclear reorganization of the HoxB locus upon induction of transcription. Genes Dev 18(10):1119-30.

Chandy M, Gutierrez JL, Prochasson P, Workman JL. 2006. SWI/SNF displaces SAGA-acetylated nucleosomes. Eukaryot Cell 5(10):1738-47.

Cosma MP, Tanaka T, Nasmyth K. 1999. Ordered recruitment of transcription and chromatin remodeling factors to a cell cycle- and developmentally regulated promoter. Cell 97(3):299-311.

De Vit MJ, Waddle JA, Johnston M. 1997. Regulated nuclear translocation of the Mig1 glucose repressor. Mol Biol Cell 8(8):1603-18.

Dieppois G, Iglesias N, Stutz F. 2006. Cotranscriptional recruitment to the mRNA export receptor Mex67p contributes to nuclear pore anchoring of activated genes. Mol Cell Biol 26(21):7858-70.

Ding WV, Johnston SA. 1997. The DNA binding and activation domains of Gal4p are sufficient for conveying its regulatory signals. Mol Cell Biol 17(5):2538-49.

Drubin DA, Garakani AM, Silver PA. 2006. Motion as a phenotype: the use of live-cell imaging and machine visual screening to characterize transcription-dependent chromosome dynamics. BMC Cell Biol 7:19.

Dundr M, Misteli T. 2003. Measuring dynamics of nuclear proteins by photobleaching. Curr Protoc Cell Biol Chapter 13:Unit 13 5.

Engebrecht J, Brent R, Kaderbhai MA. 2001. Minipreps of plasmid DNA. Curr Protoc Mol Biol Chapter 1:Unit1 6.

Entian KD. 1980. Genetic and biochemical evidence for hexokinase PII as a key enzyme involved in carbon catabolite repression in yeast. Mol Gen Genet 178(3):633-7.

Ferreira ME, Hermann S, Prochasson P, Workman JL, Berndt KD, Wright AP. 2005. Mechanism of transcription factor recruitment by acidic activators. J Biol Chem 280(23):21779-84.

Ghaemmaghami S, Huh WK, Bower K, Howson RW, Belle A, Dephoure N, O'Shea EK, Weissman JS. 2003. Global analysis of protein expression in yeast. Nature 425(6959):737-41.

Gill G, Ptashne M. 1988. Negative effect of the transcriptional activator GAL4. Nature 334(6184):721-4.

Gotta M, Gasser SM. 1996. Nuclear organization and transcriptional silencing in yeast. Experientia 52(12):1136-47.

Hampsey M. 1998. Molecular genetics of the RNA polymerase II general transcriptional machinery. Microbiol Mol Biol Rev 62(2):465-503.

Heim R, Prasher DC, Tsien RY. 1994. Wavelength mutations and posttranslational autoxidation of green fluorescent protein. Proc Natl Acad Sci U S A 91(26):12501-4.

Huang M, Zhou Z, Elledge SJ. 1998. The DNA replication and damage checkpoint pathways induce transcription by inhibition of the Crt1 repressor. Cell 94(5):595-605.

Huh WK, Falvo JV, Gerke LC, Carroll AS, Howson RW, Weissman JS, O'Shea EK. 2003. Global analysis of protein localization in budding yeast. Nature 425(6959):686-91.

Hutchison N, Weintraub H. 1985. Localization of DNAase I-sensitive sequences to specific regions of interphase nuclei. Cell 43(2 Pt 1):471-82.

Johnston M. 1987. A model fungal gene regulatory mechanism: the GAL genes of Saccharomyces cerevisiae. Microbiol Rev 51(4):458-76.

Johnston SA, Zavortink MJ, Debouck C, Hopper JE. 1986. Functional domains of the yeast regulatory protein GAL4. Proc Natl Acad Sci U S A 83(17):6553-7.

Keaveney M, Struhl K. 1998. Activator-mediated recruitment of the RNA polymerase II machinery is the predominant mechanism for transcriptional activation in yeast. Mol Cell 1(6):917-24.

Keegan L, Gill G, Ptashne M. 1986. Separation of DNA binding from the transcription-activating function of a eukaryotic regulatory protein. Science 231(4739):699-704.

Kelleher RJ, 3rd, Flanagan PM, Kornberg RD. 1990. A novel mediator between activator proteins and the RNA polymerase II transcription apparatus. Cell 61(7):1209-15.

Kim YJ, Bjorklund S, Li Y, Sayre MH, Kornberg RD. 1994. A multiprotein mediator of transcriptional activation and its interaction with the C-terminal repeat domain of RNA polymerase II. Cell 77(4):599-608.

Kipper J, Strambio-de-Castillia C, Suprapto A, Rout MP. 2002. Isolation of nuclear envelope from Saccharomyces cerevisiae. Methods Enzymol 351:394-408.

Kiseleva E, Allen TD, Rutherford S, Bucci M, Wente SR, Goldberg MW. 2004. Yeast nuclear pore complexes have a cytoplasmic ring and internal filaments. J Struct Biol 145(3):272-88.

Kolb VA, Makeyev EV, Ward WW, Spirin AS. 1996. Synthesis and Maturation of Green Fluorescent Protein in a Cell-free Translation System. Biotechnology Letters 18(12):6.

Kornberg RD. 2005. Mediator and the mechanism of transcriptional activation. Trends Biochem Sci 30(5):235-9.

Lee TI, Causton HC, Holstege FC, Shen WC, Hannett N, Jennings EG, Winston F, Green MR, Young RA. 2000. Redundant roles for the TFIID and SAGA complexes in global transcription. Nature 405(6787):701-4.

Lei EP, Stern CA, Fahrenkrog B, Krebber H, Moy TI, Aebi U, Silver PA. 2003. Sac3 is an mRNA export factor that localizes to cytoplasmic fibrils of nuclear pore complex. Mol Biol Cell 14(3):836-47.

Li X, Zhang G, Ngo N, Zhao X, Kain SR, Huang CC. 1997. Deletions of the Aequorea victoria green fluorescent protein define the minimal domain required for fluorescence. J Biol Chem 272(45):28545-9.

Lichter P, Cremer T, Tang CJ, Watkins PC, Manuelidis L, Ward DC. 1988. Rapid detection of human chromosome 21 aberrations by in situ hybridization. Proc Natl Acad Sci U S A 85(24):9664-8.

Lippincott-Schwartz J, Altan-Bonnet N, Patterson GH. 2003. Photobleaching and photoactivation: following protein dynamics in living cells. Nat Cell Biol Suppl:S7-14.

Lohr D, Venkov P, Zlatanova J. 1995. Transcriptional regulation in the yeast GAL gene family: a complex genetic network. Faseb J 9(9):777-87.

Lutfiyya LL, Iyer VR, DeRisi J, DeVit MJ, Brown PO, Johnston M. 1998. Characterization of three related glucose repressors and genes they regulate in Saccharomyces cerevisiae. Genetics 150(4):1377-91.

Ma J, Ptashne M. 1987. Deletion analysis of GAL4 defines two transcriptional activating segments. Cell 48(5):847-53.

MacPherson S, Larochelle M, Turcotte B. 2006. A fungal family of transcriptional regulators: the zinc cluster proteins. Microbiol Mol Biol Rev 70(3):583-604.

Manandhar SP, Hildebrandt ER, Schmidt WK. 2007. Small-molecule inhibitors of the Rce1p CaaX protease. J Biomol Screen 12(7):983-93.

Marmorstein R, Carey M, Ptashne M, Harrison SC. 1992. DNA recognition by GAL4: structure of a protein-DNA complex. Nature 356(6368):408-14.

Measday V, Moore L, Ogas J, Tyers M, Andrews B. 1994. The PCL2 (ORFD)-PHO85 cyclin-dependent kinase complex: a cell cycle regulator in yeast. Science 266(5189):1391-5.

Melcher K. 2000. The strength of acidic activation domains correlates with their affinity for both transcriptional and non-transcriptional proteins. J Mol Biol 301(5):1097-112.

Menon BB, Sarma NJ, Pasula S, Deminoff SJ, Willis KA, Barbara KE, Andrews B, Santangelo GM. 2005. Reverse recruitment: the Nup84 nuclear pore subcomplex mediates Rap1/Gcr1/Gcr2 transcriptional activation. Proc Natl Acad Sci U S A 102(16):5749-54.

Misteli T. 2001. Protein dynamics: implications for nuclear architecture and gene expression. Science 291(5505):843-7.

Mitchell PJ, Tjian R. 1989. Transcriptional regulation in mammalian cells by sequence-specific DNA binding proteins. Science 245(4916):371-8.

Myers LC, Gustafsson CM, Bushnell DA, Lui M, Erdjument-Bromage H, Tempst P, Kornberg RD. 1998. The Med proteins of yeast and their function through the RNA polymerase II carboxy-terminal domain. Genes Dev 12(1):45-54.

Neigeborn L, Carlson M. 1984. Genes affecting the regulation of SUC2 gene expression by glucose repression in Saccharomyces cerevisiae. Genetics 108(4):845-58.

Nonet M, Scafe C, Sexton J, Young R. 1987. Eucaryotic RNA polymerase conditional mutant that rapidly ceases mRNA synthesis. Mol Cell Biol 7(5):1602-11.

O'Brien TP, Bult CJ, Cremer C, Grunze M, Knowles BB, Langowski J, McNally J, Pederson T, Politz JC, Pombo A and others. 2003. Genome function and nuclear architecture: from gene expression to nanoscience. Genome Res 13(6A):1029-41.

Park JM, Kim HS, Han SJ, Hwang MS, Lee YC, Kim YJ. 2000. In vivo requirement of activator-specific binding targets of mediator. Mol Cell Biol 20(23):8709-19.

Perozzo MA, Ward KB, Thompson RB, Ward WW. 1988. X-ray diffraction and time-resolved fluorescence analyses of Aequorea green fluorescent protein crystals. J Biol Chem 263(16):7713-6.

Pilauri V, Bewley M, Diep C, Hopper J. 2005. Gal80 dimerization and the yeast GAL gene switch. Genetics 169(4):1903-14.

Pinkel D, Landegent J, Collins C, Fuscoe J, Segraves R, Lucas J, Gray J. 1988. Fluorescence in situ hybridization with human chromosome-specific libraries: detection of trisomy 21 and translocations of chromosome 4. Proc Natl Acad Sci U S A 85(23):9138-42.

Platani M, Goldberg I, Lamond AI, Swedlow JR. 2002. Cajal body dynamics and association with chromatin are ATP-dependent. Nat Cell Biol 4(7):502-8.

Proft M, Pascual-Ahuir A, de Nadal E, Arino J, Serrano R, Posas F. 2001. Regulation of the Sko1 transcriptional repressor by the Hog1 MAP kinase in response to osmotic stress. Embo J 20(5):1123-33.

Ptashne M. 1988. How eukaryotic transcriptional activators work. Nature 335(6192):683-9.

Ptashne M, Gann A. 1997. Transcriptional activation by recruitment. Nature 386(6625):569-77.

Ptashne M, Gann AA. 1990. Activators and targets. Nature 346(6282):329-31.

Qiu H, Hu C, Yoon S, Natarajan K, Swanson MJ, Hinnebusch AG. 2004. An array of coactivators is required for optimal recruitment of TATA binding protein and RNA polymerase II by promoter-bound Gcn4p. Mol Cell Biol 24(10):4104-17.

Rabut G, Doye V, Ellenberg J. 2004. Mapping the dynamic organization of the nuclear pore complex inside single living cells. Nat Cell Biol 6(11):1114-21.

Rose MD, Novick P, Thomas JH, Botstein D, Fink GR. 1987. A Saccharomyces cerevisiae genomic plasmid bank based on a centromere-containing shuttle vector. Gene 60(2-3):237-43.

Santangelo GM. 2006. Glucose signaling in Saccharomyces cerevisiae. Microbiol Mol Biol Rev 70(1):253-82.

Sarma N. 2007. Reverse Recruitment: A new model for eukaryotic gene regulation. Hattiesburg: The University of Southern Mississippi.

Sarma NJ, Haley TM, Barbara KE, Buford TD, Willis KA, Santangelo GM. 2007. Glucose-responsive regulators of gene expression in Saccharomyces cerevisiae function at the nuclear periphery via a reverse recruitment mechanism. Genetics 175(3):1127-35.

Schjerling P, Holmberg S. 1996. Comparative amino acid sequence analysis of the C6 zinc cluster family of transcriptional regulators. Nucleic Acids Res 24(23):4599-607.

Schmid M, Arib G, Laemmli C, Nishikawa J, Durussel T, Laemmli UK. 2006. Nup-PI: the nucleopore-promoter interaction of genes in yeast. Mol Cell 21(3):379-91.

Schwabish MA, Struhl K. 2007. The Swi/Snf complex is important for histone eviction during transcriptional activation and RNA polymerase II elongation in vivo. Mol Cell Biol 27(20):6987-95.

Sherman F. 2002. Getting started with yeast. Methods Enzymol 350:3-41.

Sil AK, Alam S, Xin P, Ma L, Morgan M, Lebo CM, Woods MP, Hopper JE. 1999. The Gal3p-Gal80p-Gal4p transcription switch of yeast: Gal3p destabilizes the Gal80p-Gal4p complex in response to galactose and ATP. Mol Cell Biol 19(11):7828-40.

Sniegowski JA, Lappe JW, Patel HN, Huffman HA, Wachter RM. 2005. Base catalysis of chromophore formation in Arg96 and Glu222 variants of green fluorescent protein. J Biol Chem 280(28):26248-55.

Sprague BL, McNally JG. 2005. FRAP analysis of binding: proper and fitting. Trends Cell Biol 15(2):84-91.

Sterner DE, Berger SL. 2000. Acetylation of histones and transcription-related factors. Microbiol Mol Biol Rev 64(2):435-59.

Stewart CN, Jr. 2006. Go with the glow: fluorescent proteins to light transgenic organisms. Trends Biotechnol 24(4):155-62.

Straight AF, Belmont AS, Robinett CC, Murray AW. 1996. GFP tagging of budding yeast chromosomes reveals that protein-protein interactions can mediate sister chromatid cohesion. Curr Biol 6(12):1599-608.

Sudarsanam P, Winston F. 2000. The Swi/Snf family nucleosome-remodeling complexes and transcriptional control. Trends Genet 16(8):345-51.

Sugase K, Dyson HJ, Wright PE. 2007. Mechanism of coupled folding and binding of an intrinsically disordered protein. Nature 447(7147):1021-5.

Taddei A, Hediger F, Neumann FR, Bauer C, Gasser SM. 2004. Separation of silencing from perinuclear anchoring functions in yeast Ku80, Sir4 and Esc1 proteins. Embo J 23(6):1301-12.

Taddei A, Van Houwe G, Hediger F, Kalck V, Cubizolles F, Schober H, Gasser SM. 2006. Nuclear pore association confers optimal expression levels for an inducible yeast gene. Nature 441(7094):774-8.

Tong AH, Evangelista M, Parsons AB, Xu H, Bader GD, Page N, Robinson M, Raghibizadeh S, Hogue CW, Bussey H and others. 2001. Systematic genetic analysis with ordered arrays of yeast deletion mutants. Science 294(5550):2364-8.

Tornow J, Zeng X, Gao W, Santangelo GM. 1993. GCR1, a transcriptional activator in Saccharomyces cerevisiae, complexes with RAP1 and can function without its DNA binding domain. Embo J 12(6):2431-7.

Treitel MA, Carlson M. 1995. Repression by SSN6-TUP1 is directed by MIG1, a repressor/activator protein. Proc Natl Acad Sci U S A 92(8):3132-6.

Triezenberg SJ. 1995. Structure and function of transcriptional activation domains. Curr Opin Genet Dev 5(2):190-6.

Tse C, Sera T, Wolffe AP, Hansen JC. 1998. Disruption of higher-order folding by core histone acetylation dramatically enhances transcription of nucleosomal arrays by RNA polymerase III. Mol Cell Biol 18(8):4629-38.

Tsien RY. 1998. The green fluorescent protein. Annu Rev Biochem 67:509-44.

Turkel S, Turgut T, Lopez MC, Uemura H, Baker HV. 2003. Mutations in GCR1 affect SUC2 gene expression in Saccharomyces cerevisiae. Mol Genet Genomics 268(6):825-31.

Vallier LG, Carlson M. 1994. Synergistic release from glucose repression by mig1 and ssn mutations in Saccharomyces cerevisiae. Genetics 137(1):49-54.

van Drogen F, Peter M. 2004. Revealing protein dynamics by photobleaching techniques. Methods Mol Biol 284:287-306.

Verkhusha VV, Akovbian NA, Efremenko EN, Varfolomeyev SD, Vrzheshch PV. 2001. Kinetic analysis of maturation and denaturation of DsRed, a coral-derived red fluorescent protein. Biochemistry (Mosc) 66(12):1342-51.

Verschure PJ, van Der Kraan I, Manders EM, van Driel R. 1999. Spatial relationship between transcription sites and chromosome territories. J Cell Biol 147(1):13-24.

Wang Y, Pierce M, Schneper L, Guldal CG, Zhang X, Tavazoie S, Broach JR. 2004. Ras and Gpa2 mediate one branch of a redundant glucose signaling pathway in yeast. PLoS Biol 2(5):E128.

Winzeler EA, Shoemaker DD, Astromoff A, Liang H, Anderson K, Andre B, Bangham R, Benito R, Boeke JD, Bussey H and others. 1999. Functional characterization of the S. cerevisiae genome by gene deletion and parallel analysis. Science 285(5429):901-6.

Wright PE, Dyson HJ. 1999. Intrinsically unstructured proteins: re-assessing the protein structure-function paradigm. J Mol Biol 293(2):321-31.

Wu J, Suka N, Carlson M, Grunstein M. 2001. TUP1 utilizes histone H3/H2B-specific HDA1 deacetylase to repress gene activity in yeast. Mol Cell 7(1):117-26.

Yeh E, Gustafson K, Boulianne GL. 1995. Green fluorescent protein as a vital marker and reporter of gene expression in Drosophila. Proc Natl Acad Sci U S A 92(15):7036-40.

Zaman Z, Ansari AZ, Gaudreau L, Nevado J, Ptashne M. 1998. Gene transcription by recruitment. Cold Spring Harb Symp Quant Biol 63:167-71.